NON-DESTRUCTIVE SASW EVALUATION OF CONTROLLED LOW STRENGTH MATERIAL AS A PIPELINE BEDDING MATERIAL

by

RATHNA PHANINDRA MOTHKURI

Presented to the Faculty of the Graduate School of

The University of Texas at Arlington

in Partial Fulfillment of the Requirements

for the Degree of

MASTER OF SCIENCE IN CIVIL ENGINEERING

THE UNIVERSITY OF TEXAS AT ARLINGTON

August 2014

To Mom and Dad……

Acknowledgements

I would first like to thank the University of Texas at Arlington for making my stay feel like home away from home. My journey here in pursuing a Master's Degree was memorable.

Deep gratitude goes to my advisor, Dr. Anand J. Puppala, for his reassuring encouragement, inspiring personality and important words of wisdom. I would also like to thank the Department of Civil Engineering and Dr. Anand J. Puppala for providing me with financial assistance throughout my study at UTA. It was, and will always be, an honor to be a student of Dr. Anand J. Puppala's. Dr. Bhaskar Chittoori gave me never-ending support and mentoring for which I am very grateful. He instilled a lot of confidence in me. I am grateful to Dr. Shih-Ho Chao and Dr. Xinbao Yu for spending their precious time serving on my committee.

I would like to thank Dr. Aravind Pedarla for his constant support and suggestions during my research work. I really appreciate his efforts. I would like to specially thank Tejo Vikas Bheemasetti for his constant support and encouragement throughout my stay at UTA. If it wasn't for him, I feel I would still be lagging behind a bit. For their friendship, invaluable suggestions and help in the laboratory, I would like to thank Spoorthi Reballi, Sadikshya Poudel, Pinit (Tom) Ruttanaporamakul, Ujwal Patil, Raju Acharya, Alejandro Pino, Ahmed Gaily, Jairo Yepes, Jorge Almendares, Humberto Johnson and Minh Tran. I also would like to thank my friends, Vikram Tej, Ranjit Balijepalli, Kartik Konda, Sindhuri Manne, Priyadarshini Subramanian, Sarmishtha Sathpathy and Pritam Karmokar for their untiring encouragement and support during my stay at UTA.

It will be incomplete if I don't thank my family for their love and support. I would like to thank my father, Jitendra Babu Mothkuri; mother, Lalitha Mothkuri and kid brother,

Rathna Surandra Mothkuri, for molding me into the person I am today. Last but not the least, I would like to thank my friends back home, Shray Badam, Pallavi Laxmikanth and Urvi Desai for their unconditional love and support.

July 17th, 2014

Abstract

NON-DESTRUCTIVE SASW EVALUATION OF CONTROLLED LOW STRENGTH MATERIAL AS A PIPELINE BEDDING MATERIAL

Rathna Phanindra Mothkuri, M.S.

The University of Texas at Arlington, 2014

Supervising Professor: Anand J. Puppala

Evaluation of stiffness properties of subsurface soil layers provides vital insight into the performance of a geotechnical entity. Stiffness properties can be determined by both field and laboratory tests. Owing to their advantages over laboratory tests, the field tests are often given priority. non-destructive seismic method Spectral Analysis of Surface Waves (SASW) has been implemented in the current research to investigate the stiffness properties of buried materials.

The SASW technique works on the principle of wave propagation. The surface wave velocity obtained through the test is used to determine the shear modulus, and thus the stiffness, of the geotechnical entity. In this study, the SASW technique has been employed to test the strength of Controlled Low Strength Material (CLSM) over time, with the main objective of assessing the quality of CLSM as a pipeline embedment material. CLSM is a mixture of native soil and water, with cement as an admixture. The main purpose of CLSM is to reduce the project expenses and increase the void filling capacity due its flowable nature. This study is a part of the Integrated Pipeline (IPL) project sponsored by the Tarrant Regional Water District (TRWD).

In order to accomplish this research objective, SASW tests were performed inside the pipeline in the prove-out section. Seventeen test sections were selected along

the length of the prove-out section, to perform the SASW tests. The prove-out section extends to a length of 500 ft. The results from these tests were analyzed using WinTFS and WinSASW software. The unconfined compression test was performed on samples obtained from the field. The samples were checked to achieve a target strength of 70 to 150 psi for CLSM after 28 days of casting, as recommended by TRWD for this study. The laboratory tests also included the resonant column test. In order to validate the field SASW results, replicate samples were cast in the laboratory, with the appropriate design mix, to perform the resonant column test. The laboratory resonant column test results were then compared with the field SASW test results for validation of field results This research paves way for future research studies on the SASW technique as an accurate measure for determining the stiffness of geotechnical entities.

Table of Contents

List of Illustrations

List of Tables

Chapter 1

Introduction

1.1 General

The study of the engineering behavior of earth materials constitutes geotechnical engineering. The necessary equipment and parameters for measurement (mainly elastic parameters) form the fundamentals of the design and analysis procedures in this field of study. In this context, the identification of elastic parameters becomes an essential part of geotechnical engineering (Murillo et al., 2013). Elastic parameters enable a geotechnical engineer in site characterization. In view of the numerous elastic properties of soil, the main focus of this research lies on shear modulus. Shear modulus is defined as the ratio of shear stress to shear strain and is denoted by *G.* Shear modulus, in general, portrays the stiffness/strength of the soil.

In the past, traditional in-situ techniques like the borehole methods were implemented to determine the shear modulus of soils. But with the passage of time, the use of geophysical seismic methods has gained much acclaim (Sheu, 1987). The geophysical seismic methods are based upon calculating the shear wave velocity of a soil without disturbing the alignment of the soil strata. The shear modulus is, in turn, derived from the calculated shear wave velocity. Rayleigh (1887) stated that the seismic wave velocity is directly related to the properties of the material in which they propagate. Transporting the soil sample from the field to the laboratory causes undesirable disturbances in the soil particle alignment, which lead to inaccurate shear modulus measurements. In addition, laboratory tests are also expensive and time consuming (Aouad, 1993). As a result, in-situ non-destructive tests are preferable over laboratory tests for the calculation of shear modulus.

In the ongoing study, investigation to assess the quality and performance of Controlled Low Strength Material (CLSM) with time was monitored with the help of the Spectral Analysis of Surface Waves (SASW) technique.

Controlled Low Strength Material (CLSM) is a mix of cement, native soil and water with the addition of additives like lime, when necessary (Chittoori et al., 2012). As the name suggests, the strength of CLSM is low when compared to that of concrete, but higher when compared to the native soil. Puppala et al. (2012) stated that the re-utilization of the native soil to form CLSM, which provides embedment to the pipeline, is economically and environmentally beneficial. The use of the excavated native soil as fine aggregate to prepare CLSM will reduce the wastage of the excavated material and will, in turn, considerably reduce the overall project expenses. This also negates the expense of importing foreign materials. Waste foundry may also be used as fine aggregate in the mix design of CLSM (Bhat and Lovell, 1996). CLSM, being a flowable fill, has the potential to fill up voids and level on its own. This induces higher strength in the CLSM layer and also induces a reduction in labor and equipment costs used for leveling purposes. In addition, the low compressive strength of CLSM, in the range of 50 to 100 psi (0.3 to 0.7 MPa), enhances future excavations (Chittoori et al., 2014). According to studies conducted by Raavi (2012), the use of native soil CLSM has met the specifications for a short-term time period. The long-term performance of CLSM is yet to be verified.

This research involves an ongoing study to address the quality and the strength-gaining capacity of CLSM. The Tarrant Regional Water District (TRWD) in collaboration with the Dallas Water Utilities (DWU) pursued the Integrated Pipeline (IPL) project to transport water from large water bodies like Lake Palestine to the Dallas/Fortworth area. The pipeline extended for a length of 150 miles and had a diameter of 9 ft. throughout. This research is mainly focused on a section of the pipeline along the J1 line. This section extends for a length

of 2 miles and is part of the 150 mile long pipeline project. TRWD considered the use of Controlled Low Strength Materials (CLSMs) as an embedment material for the pipeline construction in the Integrated Pipeline (IPL) project. CLSM was prepared by adding appropriate amounts of cement and water to the native soil. Different percentages of cement were mixed with the native soil and tested for strength over a period of time, before finalizing the mix design. As a part of this process, several studies were conducted to assess the applicability of this material. These studies revealed all of the advantages mentioned above when CLSM is used as an embedment material.

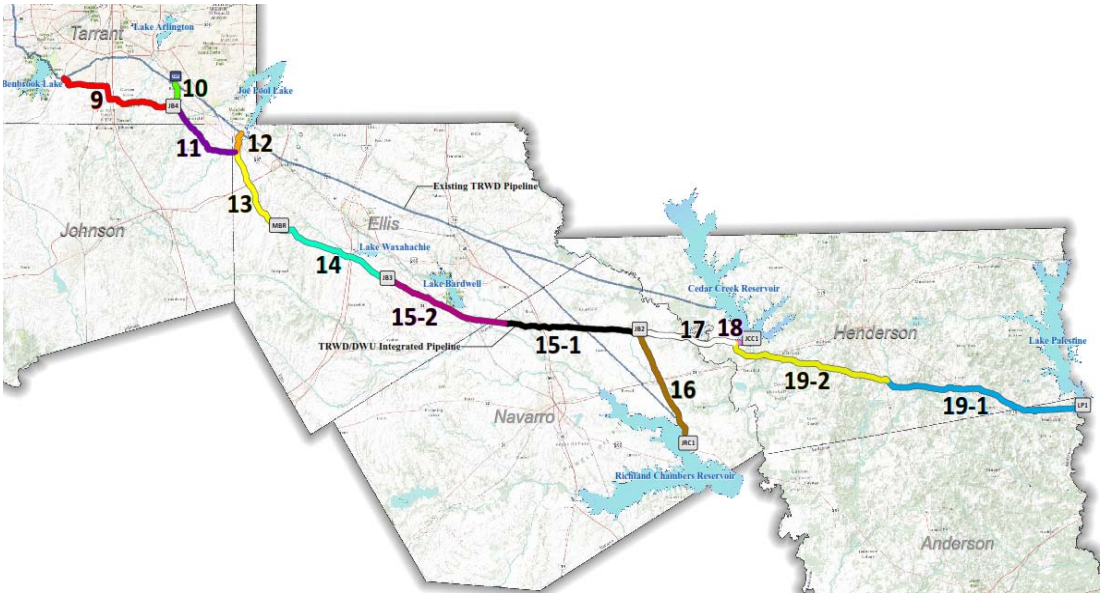

Figure 1- 1 Aerial Map of the Integrated Pipeline Project (Source: IPL Website)

1.2 Objectives

The main objectives of this research are as follows:

1. Use Spectral Analysis of Surface Wave (SASW) technique to evaluate CLSM in real field conditions and address its stiffness and strength properties.
2. The field SASW test results are compared with the laboratory resonant column test results to check for any variability.
3. Determine the strength gain of CLSM material with time

In order to achieve these objectives, the following tasks were performed during this course of study:

a. Studied the available literature on Spectral Analysis of Surface Waves (SASW) method and CLSM.
b. Conducted basic soil characterization tests on the CLSM mix, which included sieve analysis, hydrometer test, liquid limit and plastic limit tests, according to the respective ASTM standards.
c. Selected and marked points inside the pipeline to conduct SASW tests and monitor the stiffness of CLSM over time in the field.
d. Obtained CLSM samples from the field to conduct Unconfined Compression (UCS) Tests on the samples in the laboratory and, in turn, to monitor the stiffness of CLSM over time in the laboratory.
e. Performed a comparison study between the results obtained from the field and the laboratory.
f. Verified and recommended the applicability of CLSM as a pipe embedment material.

To summarize, the research tasks have been presented in the form of a flow chart in Figure 1-2.

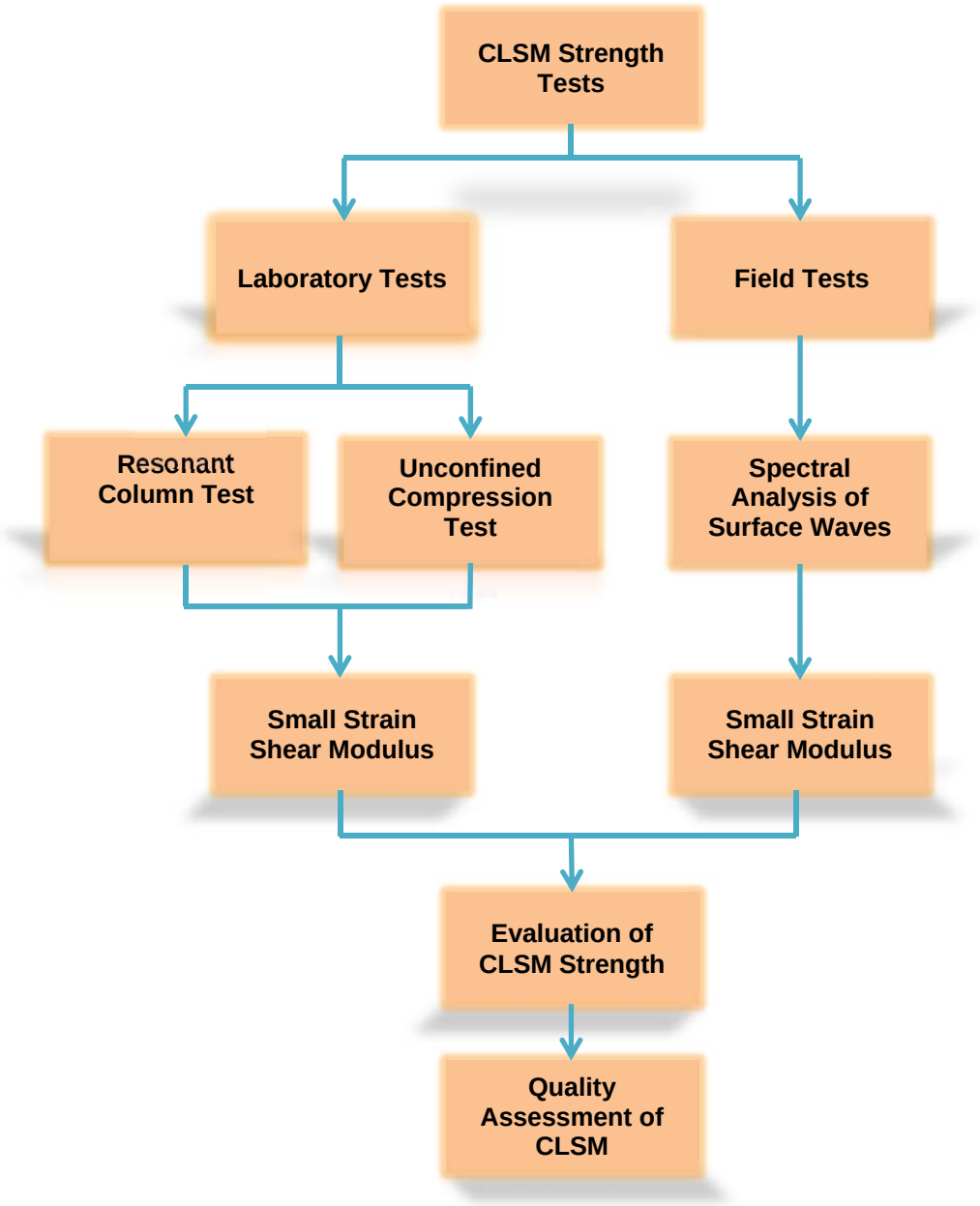

Figure 1- 2 Flow Chart Representing the Research Tasks

1.3 Organization and Summary

This thesis consists of the following six chapters:

Chapter 1 provides an introduction to shear modulus, CLSM and in-situ non-destructive seismic testing. A flow chart encompassing the research objectives of the current study is also presented in this chapter, along with the thesis organization.

Chapter 2 presents a literature review on the history and advancements in geophysical seismic testing and their types. The concept of wave propagation; classification of waves and their importance in seismic testing are also discussed in this chapter. The concept of SASW and case studies involving this technique is detailed.

Chapter 3 offers the experimental program conducted in this research. Procedures for the basic soil characterization tests, Unconfined Compression (UCS) test and the SASW test have been elucidated herein.

Chapter 4 contains the laboratory test results which include the basic soil characterization results, the unconfined compression test results and the resonant column test results.

Chapter 5 presents the SASW technique analysis procedures followed by the test results. A comparison study between the field SASW test results and the laboratory resonant column test results are also provided. Graphical analysis of an increase in shear modulus (stiffness) over time for CLSM is presented.

Chapter 6 provides a summary of the research, followed by conclusions derived from the test results. Finally, recommendations for future research are addressed.

Chapter 2

Literature Review

2.1 Introduction

In the field of geotechnical engineering, in-situ techniques have been widely implemented over the years. Their major applications include understanding material behavior through the determination of material stiffness in shear and compression (Maxwell, Fry and Ballard, 1967). The material stiffness can also be determined through laboratory tests, but, in comparison, in-situ techniques, especially non-destructive methods, proved to be more advantageous (Sheu, 1987). Two major advantages of in-situ methods over the laboratory methods are: 1. In-situ methods enable the determination of material properties under the actual stress state. 2. In the case of non-destructive methods, the in-situ methods do not require sample extraction, and thus eliminate the possibility of any discrepancies in the calculation of material properties. According to Groves (2010), in-situ methods, which do not disturb the homogeneity of the soil in the process of testing, were termed as non-destructive in-situ methods. Non-destructive in-situ methods are diverse in nature, but the main focus of this study is on non-destructive seismic methods.

Non-destructive seismic methods use the propagation of elastic waves (mostly surface waves) generated by an impulse on the surface, to determine the material characteristics. Elastic waves are broadly classified into two types: 1. body waves, 2. surface waves. Seismic methods use surface waves for their study (Nazarian, 1984).

The first implementation of the surface wave method (also known as seismic method) dates back to as early as the 1950s. Jones (1951) performed experimental studies on the use of surface wave velocity to monitor changes. Henkelom (1962) and Klomp (1962) used steady-state vibrations to perform surface wave tests. Unfortunately, neither of these two studies provided any theoretically correct solution (Sheu, 1987). In the years to follow, further

studies on the steady-state surface wave were improvised by Ballard (1964), Maxwell and Fry (1967), Ballard and Casagrande (1967) and Cunny and Fry (1973). These studies focused on the use of the steady-state wave as a reliable factor for use in determining the modulus profiles of geotechnical systems, mainly soils and dams. It was later in the 1980s, when Heisey et al. (1982), and Nazarian and Stokoe (1984) developed a theoretical solution for the surface wave method and used the method to evaluate pavements. Studies by Nazarian et al. (1993) yielded the development of an analyzer that performs the field test in a fully automated manner. This carved the path for later studies by Aouad et al. (1993), Joh (1996), Stokoe and Santamarina (2000), Cho and Lin (2001) and Suharsono et al. (2004) which developed the surface wave method to the present SASW (Spectral Analysis of Surface Wave) method.

This chapter further presents a brief overview of the wave propagation theory and the different seismic methods in use, mainly SASW.

2.2 Theory of Wave Propagation

An impact on the surface of an engineering material generates disturbances in the material. These disturbances are generated due to the propagation of stress (seismic) waves within the body of the medium. The waves can be distinguished as two waves, P-wave (compression) and S-wave (shear). These waves are collectively termed as body waves because they propagate within the body of the whole space. A new type of waves that propagated along the surface of the body was identified by Rayleigh in 1885. These were termed Rayleigh waves, after the name of their founder. The characteristics of each of the above mentioned waves are discussed hereafter.

2.2.1 Body Waves

Body waves, as mentioned above, are categorized into P-waves and S-waves, depending on the direction of their propagation. In P-waves, the particle motion is in the

direction of propagation of the waves. On the contrary, in S-waves, the particle motion is perpendicular to the direction of propagation of the wave. The directions of P-waves are always longitudinal and that of S-waves are transverse; hence, the names compression and transverse waves, respectively. This is displayed in Figure 2-1.

Due to the particle motion in P-waves, its velocity is higher than that of S-waves. The velocities of the compression waves (V_P) and shear waves (V_S) can be determined by the following equations:

$$V_P = \sqrt{\frac{M}{\rho}} = \sqrt{\frac{E}{\rho} * \frac{(1-\upsilon)}{(1-2\upsilon)(1+\upsilon)}} \quad (2.1)$$

$$V_S = \sqrt{\frac{G}{\rho}} = \sqrt{\frac{E}{\rho} * \frac{1}{2(1+\upsilon)}} \quad (2.2)$$

$$\frac{V_P}{V_S} = \sqrt{\frac{2(1-\upsilon)}{(1-2\upsilon)}} \quad (2.3)$$

Where: M = constrained modulus,

G = Shear modulus,

E = Young's modulus,

v = Poisson's ratio, and

ρ = mass density (total unit weight divided by the acceleration due to gravity).

Equations 2.1 and 2.2 were given by Graff (1991) and Equation 2.3 was given by Keary et al. (2002). Considering a Poisson's ratio value of 0.25, V_S is approximately equal to $0.59V_P$ (Groves, 2010). Therefore, it can be said that S-waves have smaller wavelengths than P-waves. It has been estimated that approximately 7% of the energy in a wave front

generated by a point source in a solid material is P-wave energy, and approximately 26% of the energy generated is S-wave energy (Miller and Pursey, 1955).

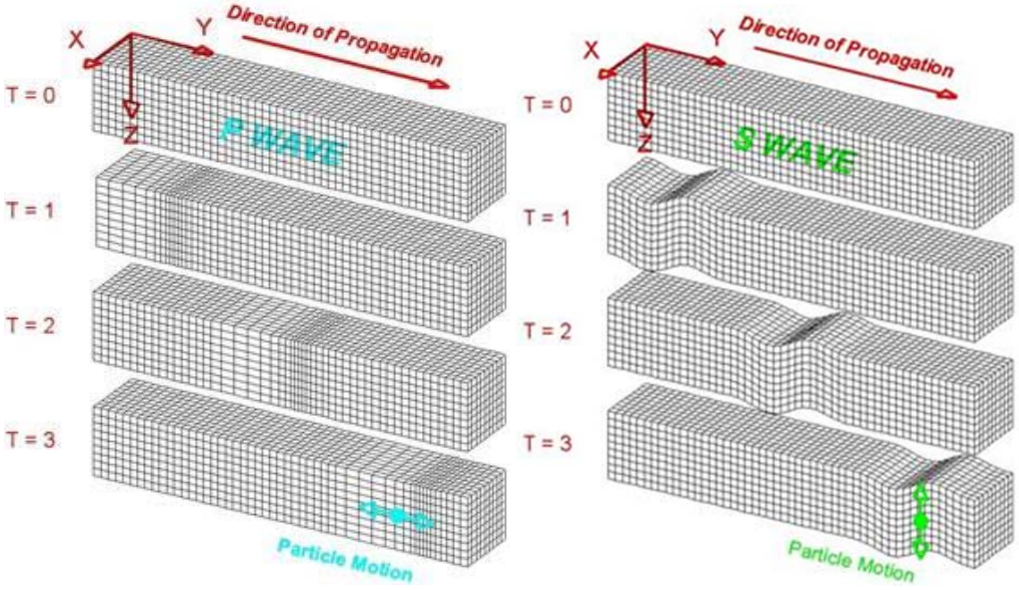

Figure 2- 1 Propagation of Body Waves (Braile, 2006)

2.2.2 Surface Waves

While P-waves and S-waves travel within the body of the elastic medium, other types of waves, which travel along the surface of the medium, can be generated. These are termed as surface waves. Surface waves are classified into two types: Rayleigh waves and Love waves.

Rayleigh, in 1885, was the first to identify waves that propagate along the surface of a uniform half-space; hence, Rayleigh waves were discovered. A noticeable trait of these waves was that they decay exponentially with depth. They spread out in a two-dimensional cylindrical pattern (radius r). This causes their amplitude to diminish with travel time from the source proportional to $1/\sqrt{r}$. The particle motion in Rayleigh waves is a combination of that of P-waves

and S-waves, hence forming a retrograde elliptical motion. Due to these properties of Rayleigh waves, many researchers used them to determine the layer stiffness of the upper layers of the crust. They are also responsible for causing significant damage in times of an earthquake. The Rayleigh wave velocity is a function of Poisson's ratio, but, for simplicity purposes, it is approximated as being equal to nine-tenths of the shear wave velocity. Figure 2-2 shows the propagation of Rayleigh waves. In a homogeneous medium, the Rayleigh wave velocity does not change with frequency; i.e., waves with different wavelengths travel at the same speed. However, in a layered medium, Rayleigh wave velocities vary with frequency (Aouad, 1993). This characteristic is called dispersion and forms the principle of the SASW method.

The other type of surface waves, as mentioned above, is Love waves. These waves exist only in the presence of a low-velocity surface layer overlying a high velocity layer. These waves were named after a researcher named Love. Love, in 1991, demonstrated that these waves are a result of multiple reflections between the top and bottom of the low-velocity layer (Aouad, 1993). The particle motion of Love waves is both horizontal and transverse to the direction of wave propagation. Figure 2-2 shows the propagation of Love waves.

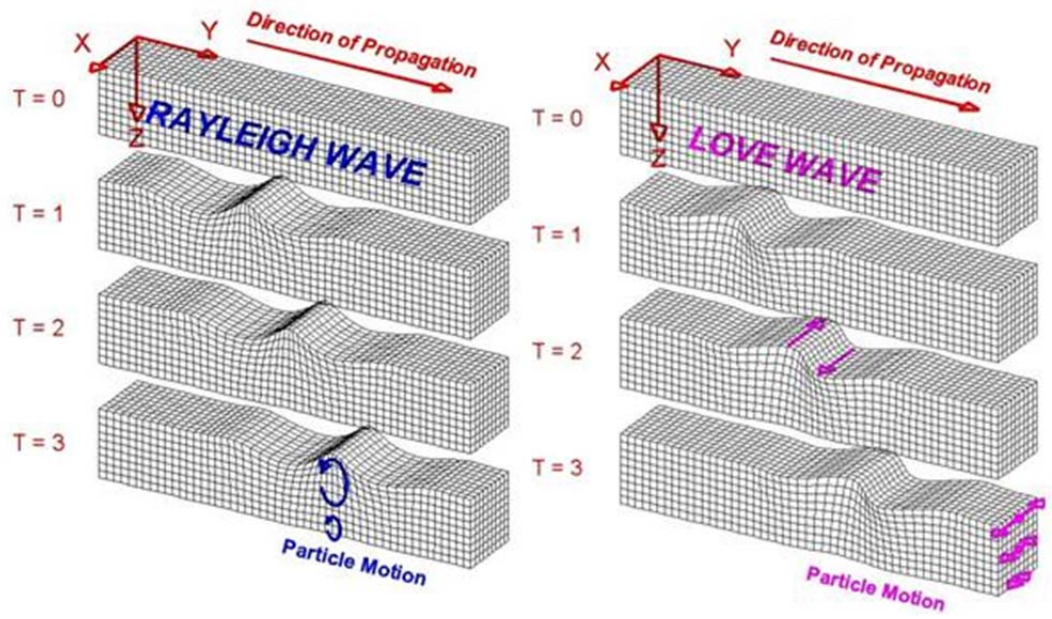

Figure 2- 2 Propagation of Surface Waves (Braile, 2006)

2.2.2.1 Relation between Rayleigh Wave Velocity and Shear Wave Velocity

Shear wave velocity profiles provide some valuable information which has been used by many engineers, geologists and seismologists to better understand the engineering properties of geotechnical sites for the purpose of making their designs safer and more reliable. A good example is that the shear wave velocity profile is directly related to the stiffness of a soil profile; thus, the thickness of the different strata forming the soil profile may be determined (Nazarian, 1984). Shear wave velocity also helps in calculating the shear modulus and Young's modulus, which play a major role in geotechnical engineering. In the recent past, structural engineers also adopted the use of shear wave velocity profiles in their studies.

Rayleigh waves are important in determining the stiffness of a geotechnical engineering entity because shear wave velocity can be easily derived from the Rayleigh wave

velocity (Aouad et al., 1993). This is one of the reasons why SASW measurements have become so popular over time, the other reasons being cost-effectiveness and the non-destructive nature of testing. Richart et al. (1970) gave a theoretical relationship between Rayleigh waves and shear waves propagating in an elastic half space:

$$\left(\frac{V_R}{V_S}\right)^6 - 8\left(\frac{V_R}{V_S}\right)^4 + \left(24 - 16\left(\frac{(1-2\upsilon)}{(2-2\upsilon)}\right)\right)\left(\frac{V_R}{V_S}\right)^2 + 16\left(\left(\frac{(1-2\upsilon)}{(2-2\upsilon)}\right) - 1\right) = 0 \qquad (2.4)$$

V_R denotes Rayleigh wave velocity and V_S denotes shear wave velocity. Cheng (2007) plotted the relationship between V_R and V_S with respect to the Poisson's ratio (υ), as shown in Figure 2-3. From the figure, the ratio of V_R to V_S ranges from 0.875 to 0.955 for a Poisson's ratio value ranging from 0 to 0.5 respectively (Cheng, 2007). This implies that the maximum error that could occur in estimating the value of V_S from V_R, with an improper Poisson's ratio value, was not more than 10%. This was depicted in the form of a simple equation as follows:

$$0.874 < \frac{V_R}{V_S} < 0.955 \qquad (2.5)$$

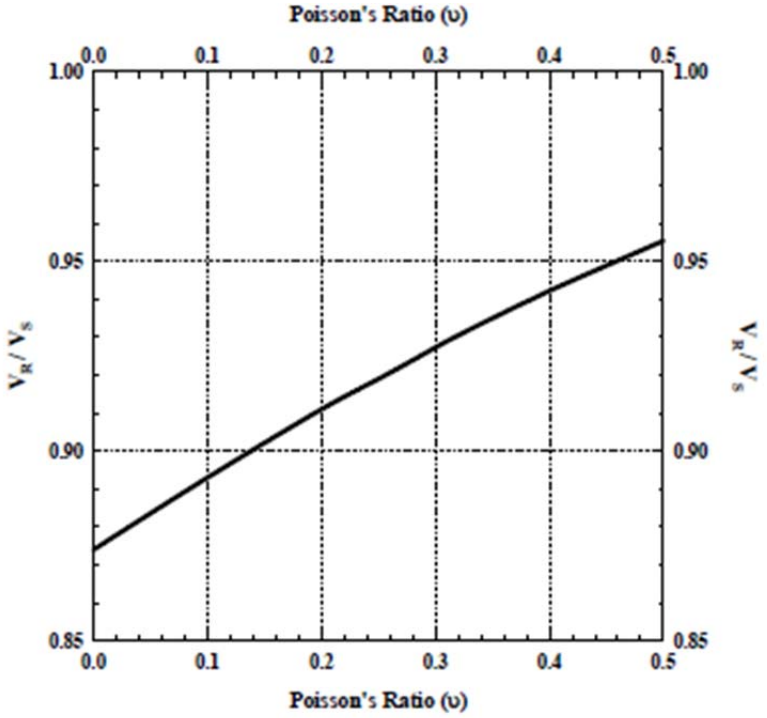

Figure 2- 3 Variation of the Ratio of Rayleigh Wave to Shear Wave Velocity with Poisson's Ratio (Cheng, 2007)

2.3 In-Situ Seismic Techniques

Seismic methods, also known as geophysical methods, are almost always nondestructive and do not require a borehole for conducting the test. These techniques are commonly used to image the subsurface of the earth in support of transportation-related geotechnical investigations (Sirles, 2006). A few commonly employed methods include seismic refraction, common offset seismic reflection, Multi-channel Analysis of Surface Waves (MASW), Spectral Analysis of Surface Waves (SASW), Refraction microtremor (ReMi), Ground Penetrating Radar (GPR), Electromagnetic method (EM), electrical resistivity, Induced Polarization (IP), magnetics, Self Potential (SP) and gravity (Wightman et al., 2004; Anderson, 2006).

2.3.1 Seismic Refraction

In this method, low frequency pulses of seismic energy are emitted by a seismic source, such as a hammer-plate or a weight drop. The type of source is selected based upon the local field conditions and the required depth of penetration. For applications necessitating a deeper depth, explosives may be used within the constraints of the environmental regulations (Redpath, 1973).

The seismic waves propagate downward through the ground until they are reflected or refracted off the subsurface layers (Sharma, 1997). These refracted waves are detected by arrays of 24 or 48 geophones spaced at regular intervals of 1-10 meters, depending on the desired depth of penetration. Sources can be positioned at either end of the array, depending on the requirement of forward and reverse wave arrivals along the array.

2.3.2 Refraction Microtremor (ReMi)

Refraction Microtremor (ReMi) is a surface-wave seismic method for estimating in-situ shear wave (from Rayleigh wave) velocities down to depths of 100 meters. This technique provides a non-invasive way of obtaining a vertical shear wave profile, similar to that of MASW (Louie, 2001).

A linear array of multiple (usually 24 or 48) equally-spaced geophones is established and connected to a seismograph in order to obtain the ReMi dispersion curve of the surface Rayleigh waves. The length of the array depends on the depth to which an investigation is desired (Rosenblad et al., 2009). The length of the array should be approximately three times the depth of investigation; i.e., in order to obtain information for 30 meters (100 feet) depth, a length of 300 feet or more is necessary (Liu et al., 2005). So, once the linear array is established, Spectrum records both the ambience and active-source noise recordings. The shorter duration recordings are for shallow depth information, and the longer duration

recordings are associated with the deeper depth information (Rosenblad et al., 2009). These noise recordings are then processed using SeisOpt® ReMi™ software, developed by Optim of Reno, Nevada.

First, a slowness-frequency wave-field transformation is applied to each of the noise recordings. This yields a slowness-frequency spectral image (Merino et al., 2012). Once this image is generated, the "fundamental mode" dispersion curve of the Rayleigh wave is then chosen. This is done by selecting the minimum phase velocity of the envelope of Rayleigh wave energy, which is in correlation with the waves that are travelling parallel to the array. Then, an iterative forward modeling process is applied to generate an optimal velocity-depth profile that would produce the selected dispersion curve. Velocity here refers to shear wave velocity. The end product of the ReMi technique is a one-dimensional column of shear wave velocity for each seismic line established at the site.

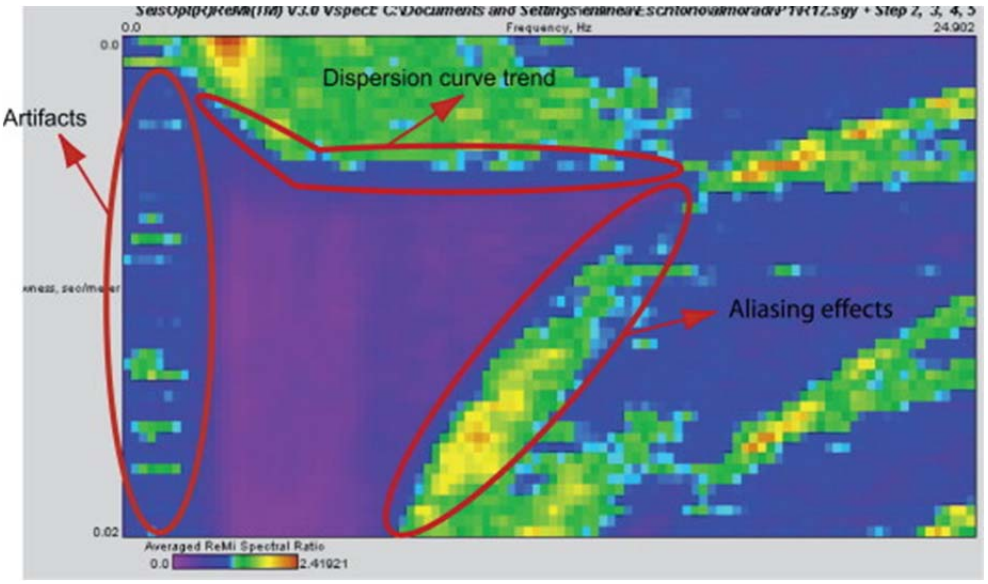

Figure 2- 4 Example of slowness-frequency image obtained through the ReMi technique (Merino et al., 2012)

2.3.3 Ground Penetrating Radar (GPR)

Ground Penetrating Radar (GPR) is a geophysical method that studies the reflections of electromagnetic signals produced by a transmitter antenna and collected by a signal receiver, located in a lightweight portable device (Pyakurel et al., 2008). The frequency of these electromagnetic signals is high (ranging from 20 MHz to 1 GHz). This yields very high resolution in the study (Nuaimy et al., 2000). However, the depth of penetration is limited to only a few meters (Annan and Chua, 1988).

The GPR test starts with the slip of the antenna on the ground. This enhances a real time signal registration (commonly known as radargram) on the screen. The maximum amplitudes correspond to the signal reflected from terrain discontinuities, such as archaeological remains, presence of any voids and lithological changes. Thus, this technique is often used in locating cavities, archaeological remains and tunnels in the subsurface (Appel et al., 1997). Figure 2-5 depicts a radargram. The major drawback of this method is that its use is limited to very low depths.

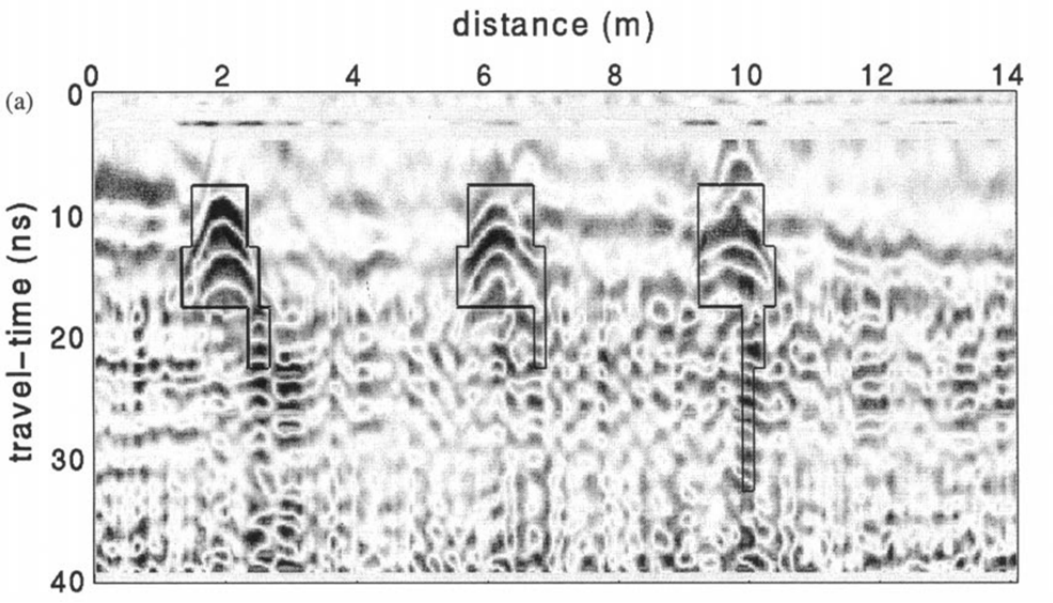

Figure 2- 5 Example of a Radargram showing 3 Pipes (Nuaimy et al., 2000)

2.3.4 Electromagnetic Method (EM)

The Electromagnetic method, also known as the Electromagnetic Terrain Conductivity method, measures the conductivity of earth materials, buried objects and backfill utilizing electromagnetic induction (Koerner et al., 1985). Measurements can be made either in the time domain or the frequency domain. While some tools are used to locate metals in the subsurface, others are used to create conductivity-depth models of the subsurface.

The concept of electromagnetic induction is that current will flow through the conductor in response to the electromotive force (Lopes, 1994). The plane of flow of current in the conductor is perpendicular to the lines of the magnetic field of force from the transmitter. Thus, current flow within the conductor generates a secondary magnetic field, whose lines of force oppose that of the primary magnetic field at the conductor. Hence, the receiver coil, which is at a small distance from the transmitter coil, is energized by the field from the transmitter and by the induced currents in the ground.

2.3.5 Electrical Resistivity Method

The Electrical Resistivity method is a geophysical method used to infer subsurface structure based on the variation in electrical resistivities of different geological materials (Groves, 2010). The principle of the electrical resistivity method is that the distribution of electrical potential in the ground, around a current-carrying electrode, depends on the electrical resistivities of the surrounding soils and rocks. The test involves the application of an electrical current (DC) between two electrodes which are implanted in the ground to measure the potential difference between two additional electrodes that do not carry current (Keary et al., 2002). All four electrodes are placed in a line on the surface, with the potential electrodes in the middle and the current electrodes to the edges. The current used is either DC or low frequency AC (approximately 20 Hz). The analysis is usually done on the basis of direct currents.

2.3.6 Induced Polarization (IP)

Induced polarization was first reported by Conrad Schlumberger (Dobrin, 1960). He termed it “provoked polarization.” While performing resistivity tests, it was observed that the potential difference between the electrodes did not drop instantaneously to zero when the current was turned off, but slowly decayed over a period of time to drop to zero (Schlumberger, 1932). This implied that the ground could be electrically polarized to form a battery, when energized with an electric current.

Two types of IP data may be acquired: frequency domain and time domain. Frequency domain data is generated by observing the effect of alternating currents on the measured value of resistivity (Bleil, 1948). Time domain data is generated by deciphering the portions of the earth where current flow is maintained for a short time after the termination of the applied current. The IP method is often used in exploration of ore bodies and groundwater, but has limited use otherwise. Figure 2-6 shows the test setup of the method.

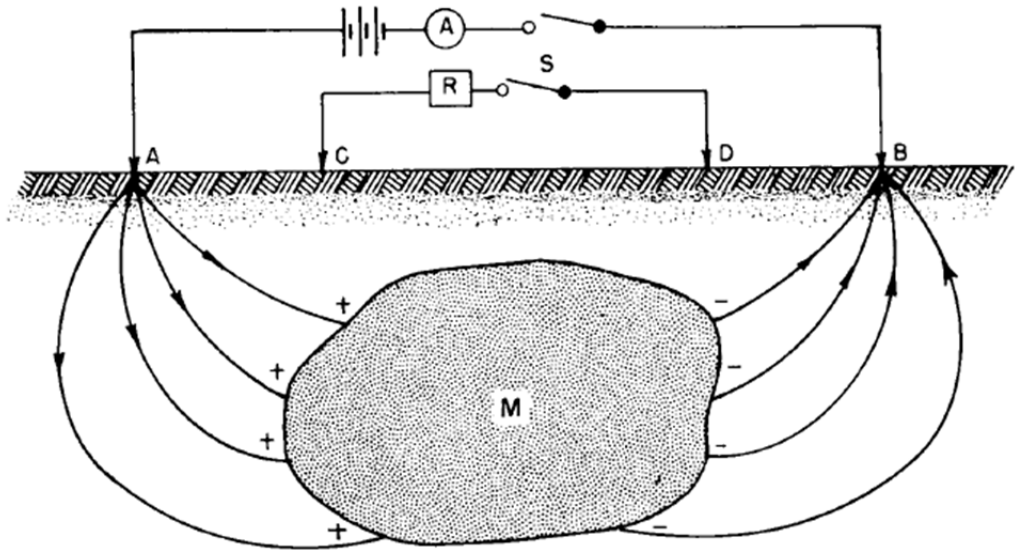

Figure 2- 6 Test setup of the Induced Polarization method (Bleil, 1948)

2.3.7 Self Potential (SP) Method

The Self Potential method is conducted primarily to measure the ambiguities present in the groundwater. It is used to measure the potential differences arising from an oxidation - reduction of metallic bodies that pollute the water table (Lang, 1970). It also enhances the measurement of streaming potential associated with the flowing groundwater. The Self Potential method is often conducted to determine the zones of seepage in earth-filled dams and levees. Also, the SP method is qualitative in nature; it does not try to quantify the anomaly's volume. Figure 2-7 depicts a schematic of the method.

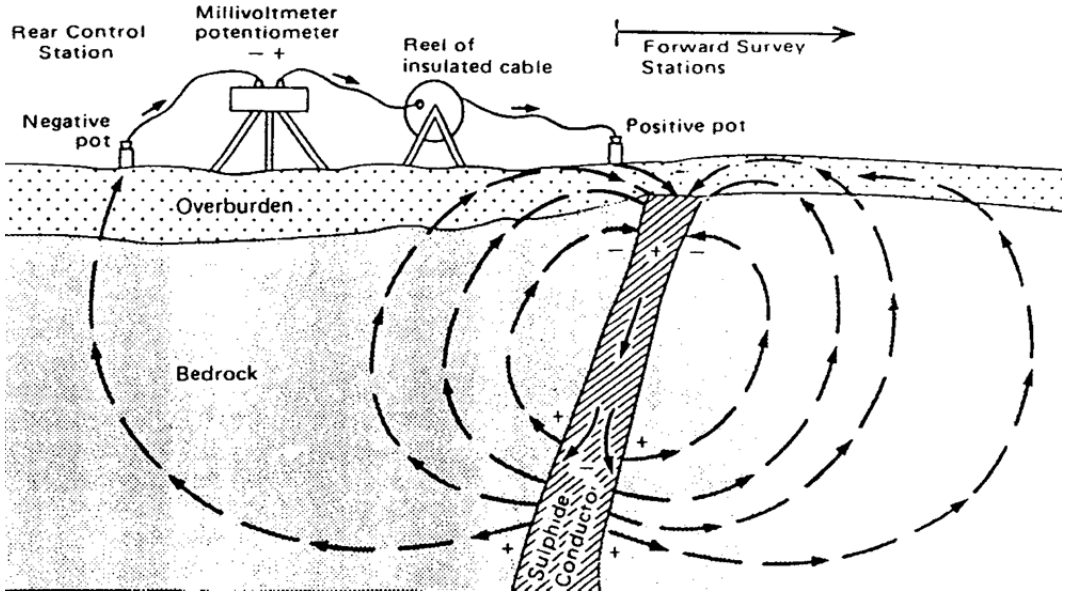

Figure 2- 7 Schematic of the Self-Potential method (Lang, 1970)

2.3.8 Magnetic Method

The Magnetic method is used to detect buried magnetic and ferrous objects, such as drums; and geological structures, such as igneous dikes, that cause ambiguities in the earth's

magnetic field (L.J. Peters, 1949). Thus the sole purpose of this technique is to identify magnetic-susceptible entities in the earth's structure that may cause future anomalies. In a few cases, magnetic data may be interpreted quantitatively and transformed into a constrained geologic model (Hansen et al., 1993).

2.3.9 Gravity Method

A study of detailed gravity data enables a better understanding of the subsurface geology (Hoffman, 1997). The gravity method is non-intrusive, as well as passive, in nature; i.e., energy need not be transmitted into the ground surface to acquire data (Meyer et al., 1995). This method involves a portable device, thus making it ideal for use in any area. The gravity data provides information about densities of rocks underground.

2.3.10 Multi-Channel Analysis of Surface Waves (MASW)

The most common objective of Multi-channel Analysis of Surface Waves (MASW) is to provide assistance with mapping variations in the shear wave velocities with respect to depth. This can also be termed as depth profiling. A seismic velocity panel is generated from the calculated shear wave velocities at the desired depth, along a seismic survey line (Lai and Wilmanski, 2005). The analysis of this geophysical method is based on the dispersion of surface waves, generally Rayleigh waves.

The Rayleigh wave energy generated, using an acoustic source, is recorded at predetermined receiver locations (Nazarian and Stokoe, 1984). This data is used to generate a dispersion curve (phase velocity versus frequency). The dispersion curve is then inverted and analyzed to generate a one-dimensional shear wave velocity profile. Two-dimensional and three-dimensional models can also be generated if additional MASW data sets are available from the adjacent locations. Figure 2-8 depicts the schematic of the test setup.

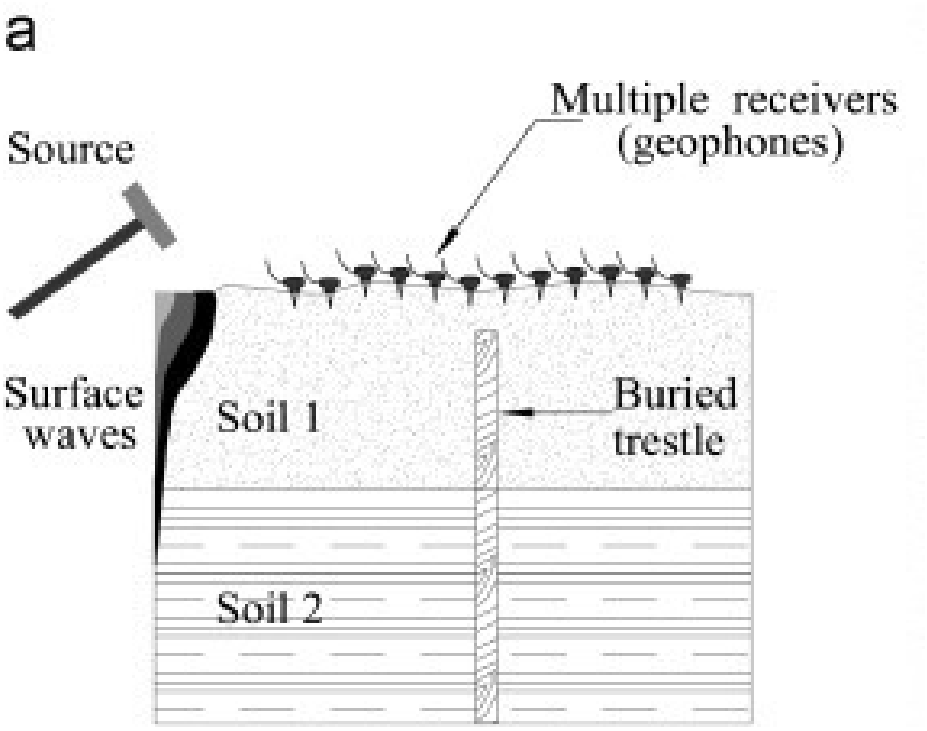

Figure 2- 8 Schematic of MASW method (Tallavo et al., 2008)

2.4 Spectral Analysis of Surface Waves (SASW)

The Spectral Analysis of Surface Waves (SASW) method is a relatively new in-situ non-destructive seismic method for determining the shear wave velocity profiles of a given geotechnical entity. The principle behind the SASW method is in calculating the dispersive characteristic of Rayleigh waves when travelling through a layered medium. Longer wavelengths penetrate deeper and are thus affected by the material properties at great depths. Rayleigh wave velocity is then converted to shear wave velocity through correlations, and, ultimately, the shear modulus of the soil is attained.

Van der Pol (1951) and Jones (1955) were the first to use the concept of surface waves in the implementation of the Steady-State method. The drawback of the Steady-State method lies in assuming that the detected wave signal is from the Rayleigh wave. In other

words, all the other types of waves are ignored. In the early 80s, a two-receiver approach was introduced by researchers from The University of Texas, Austin, which was based on Fast Fourier Transform (FFT) of phase spectra generated by surface waves, with the help of an impact. This method has been widely known as Spectral Analysis of Surface Waves (SASW) (Heisey et al., 1982). An analytical model for the surface wave method was developed by Nazarian and Stokoe (1984), with the intention of making the method theoretically correct. The theoretical study was further enhanced by Sanchez-Salinero et al., in 1987. Tokimatsu et al. (1991), in the meantime, refined the soil site inversion theory. A modern computer approach was later developed by Martincek (1994). Works by Rix et al. (1991), Gucunski and Woods (1992), Aouad (1993), Stokoe et al. (1994) and Ganji et al. (1998) further enhanced the surface wave method to its present stature.

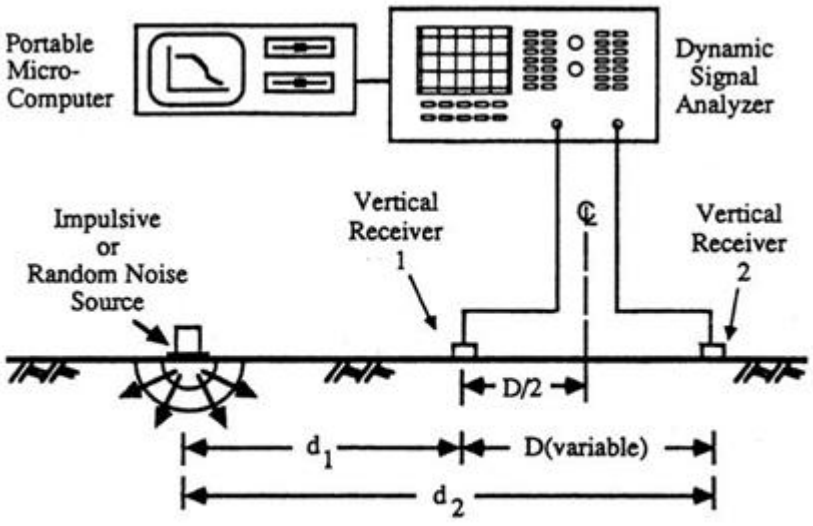

Figure 2- 9 Test setup of SASW method (Rix et al., 1991)

In the current research, the SASW technique was adopted in the determination of strength development of CLSM manufactured from native backfill. Hence, studies related to SASW testing are highlighted in the following context.

2.4.1 Case Studies and Applications of SASW Method

The Spectral Analysis of Surface Waves (SASW) method has diverse applications in the field of geotechnical engineering. A few of them have been discussed with the help of case studies.

2.4.1.1 Application of SASW Method for Rock Mass Characterization (Goh et al., 2011)

The main objective of this article was to determine the Rock Quality Designation (RQD) value and to conduct an excavation classification analysis, using the SASW method. RQD portrays the overall rock mass quality (Deere, 1968). According to Deere (1964), RQD may be calculated as follows:

$$RQD = \frac{Cumulative\ core\ length{>}100mm}{\text{Total drilling length}}(100) \qquad (2.6)$$

Suharsono et al. (2004) proposed the determination of RQD, using shear wave velocities derived from the SASW method. This is shown by the following equation:

$$RQD\ (percent) = 100^{(1-\delta)} \qquad (2.7)$$

$$\text{where: } \delta = \left(\frac{(V_{S\mu}-V_{S\beta})^2}{(V_{S\mu}+V_{S\beta})^2}\right)^2 \qquad (2.8)$$

Figure 2-10 illustrates the locations of the test, and Table 2-1 depicts the classification of rock mass based on the RQD values (Deere, 1968).

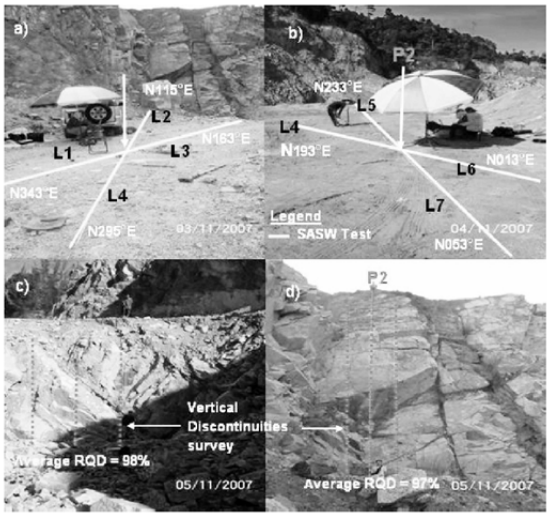

Figure 2- 10 Testing Locations (Goh et al., 2011)

Table 2- 1 Rock mass classification based on RQD (Deere, 1968)

No.	RQD (percent)	Rock Mass Quality
1	0-25	Very Poor
2	25-50	Poor
3	50-75	Fair
4	75-90	Good
5	90-100	Excellent

RQD values were calculated by improvising discontinuity surveys (traditional methods) as well as by the SASW method. For the SASW method, five test locations were selected and four SASW tests were conducted at each station. Thus, a total of 20 SASW tests were conducted. Samples from these five stations were collected and tested in the laboratory. The average ultrasonic shear wave velocity ($V_{s\mu}$) obtained from the standard laboratory tests on the five core samples was 3365 m/s. The results yielded from these tests are illustrated in Table 2-2.

Table 2- 2 Calculated boundaries for Excavation Classification (Suharsono, 2006)

RQD (percent)	Excavation Classification	$Y=V_{S\beta}/V_{S\mu}$	Boundary for $V_{S\beta}$ (m/s)
90-100	Blasting	0.3348	1127
75-89	Hydraulic Breaking	0.2488	837
50-74	Hard Ripping	0.1883	634
25-49	Easy Ripping	0.1486	500
0-24	Digging	0	0

From this study, it was concluded that the difference between the RQD values derived from the SASW tests and those of discontinuity surveys was less than 10 percent. Because of this small margin of error, Goh et al. (2011) stated that the SASW test is an alternative method for the determination of RQD.

2.4.1.2 Nondestructive Evaluation of In-Place Cement Mortar Compressive Strength using SASW (Cho et al., 2005)

The main purpose of this research was to compare and correlate the surface wave velocity with the mortar compressive strength, using the SASW method. To cross check the results, three different testing methods were implemented: SASW, resonant frequency and the cylinder test.

The test procedure involved the preparation of two 3000 psi and one 2000 psi cement mortar slab specimens. Mortar slabs were chosen for this study because mortar is more homogeneous than concrete. The size of each specimen was 3' x 3' x 4". SASW tests were conducted on these specimens.

The SASW test setup involves a source and two receivers. The source and the receivers were placed on the cement mortar slabs so that the distance between the source and the first receiver was equal to the distance between the first receiver and the second receiver. Figure 2-11 illustrates the test setup.

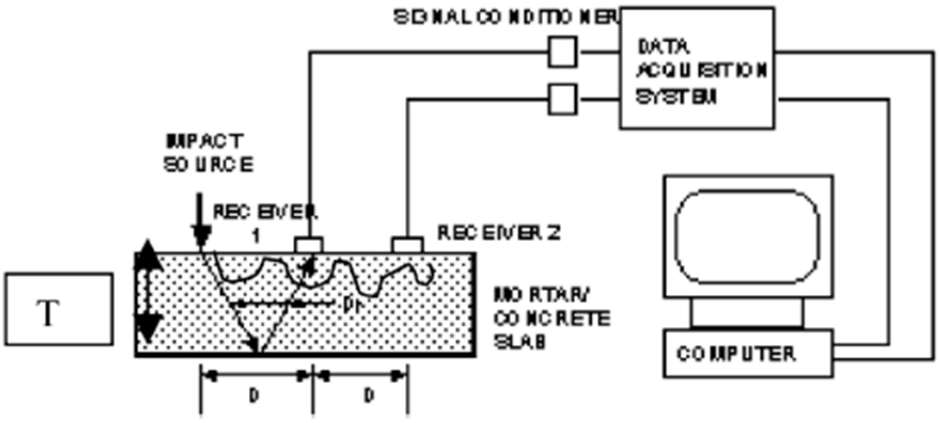

Figure 2- 11 SASW test setup (Cho et al., 2005)

A modified SASW approach was improvised in this study to eliminate the effects of boundary reflections. In this new technique, each of the three slab specimens was tested at 9 positions, evenly spaced, and a minimum of 6'' away from the boundaries of the slab. Each position in the same specimen, having the same compressive strength, was expected to produce a similar result.

The implementation of the modified SASW approach yielded the following results, which are illustrated graphically in Figure 2-12.

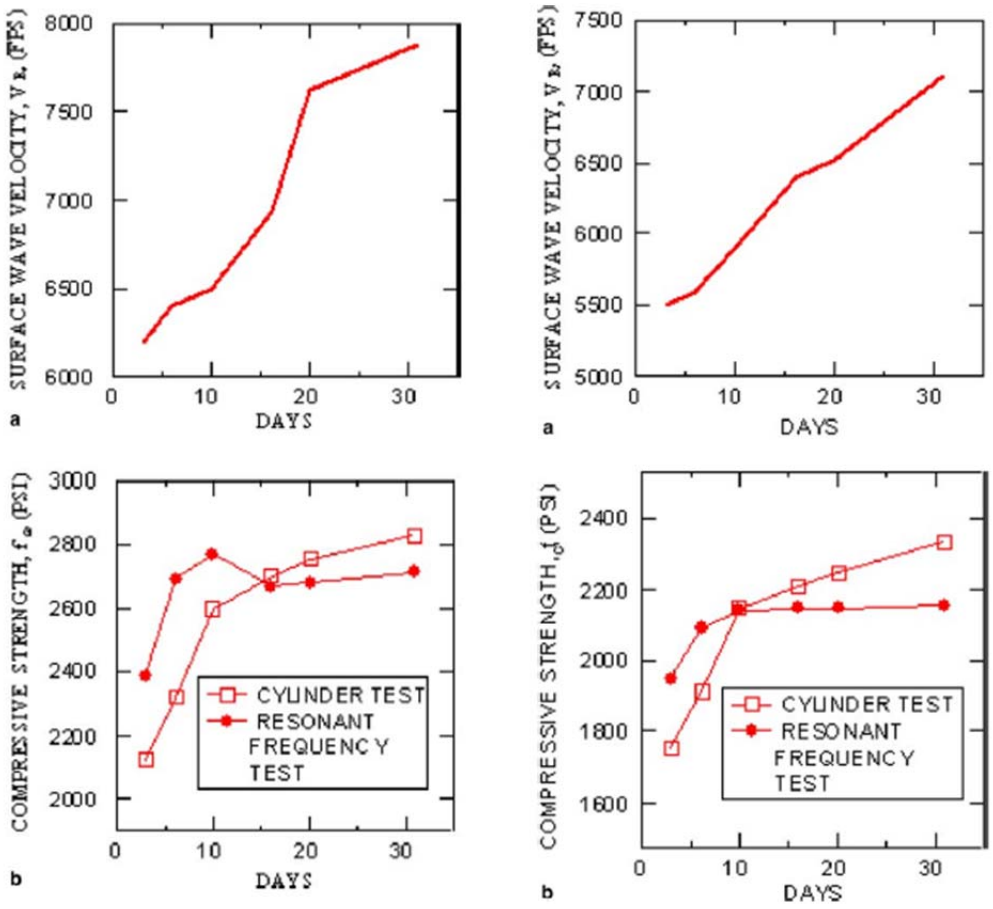

Figure 2- 12 Surface wave velocity and compressive strength at different ages of 3000 psi specimens (left) and 2000 psi specimens (right) (Cho et al., 2005)

Figure 2-13 illustrates a summary plot which was developed to demonstrate the correlation between surface wave velocity and mortar compressive strength for the 2000 psi and 3000 psi specimens.

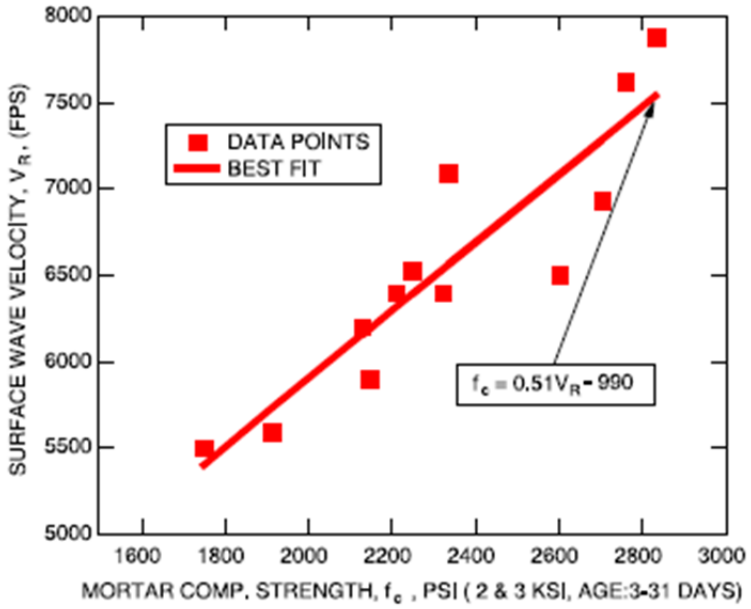

Figure 2- 13 Plot to demonstrate the correlation between shear wave velocity and mortar compressive strength (Cho et al., 2005)

Thus Cho et al. (2005) concluded that the problems associated with the boundary reflection effects were eliminated by using only the signals before the time when the reflected compression waves reach the near receiver from the source. Through this modification, an accurate dispersion curve was generated.

2.4.1.3 SASW Method to assess Shear Wave Velocity within Centrifuge Models (Murillo et al., 2009)

The objective of this research was to evaluate the SASW technique for reduced scale centrifuge models by comparing the centrifuge wave propagation results with laboratory

measurements. In order for the laboratory results to be comparable to those on the field, Bender elements were used in the laboratory.

Three models were considered in performing these tests. The soil properties of these models are given in the following table.

Table 2- 3 Soil Properties (Murillo and Thorel, 2004)

Mixture		Standard Proctor		French Road Classification System
Kaolin (%)	Sand (%)	W_{opt} (%)	Γ_d (kN/m^3)	
100	0	29.3	14.4	A3
35	65	11.5	19.6	B6
12	88	14.4	18.5	B31

The test results for the three models are illustrated in the following graphs.

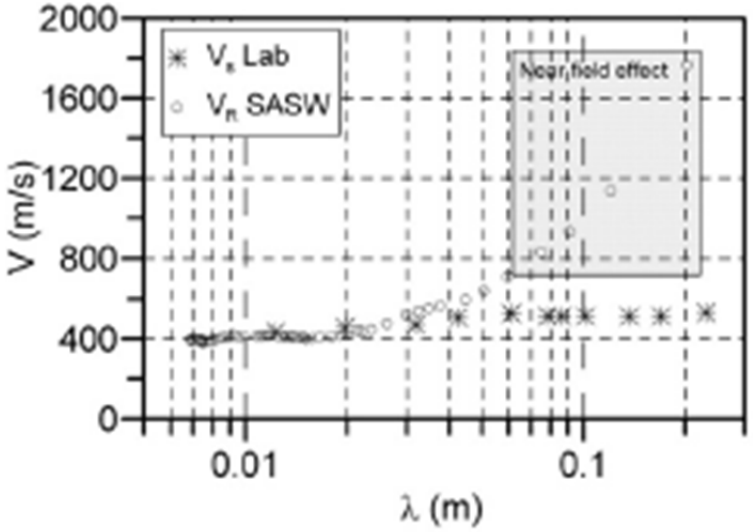

Figure 2- 14 Comparison of shear wave velocities obtained from the centrifuge and laboratory test for Model A (B31) (Murillo et al., 2009)

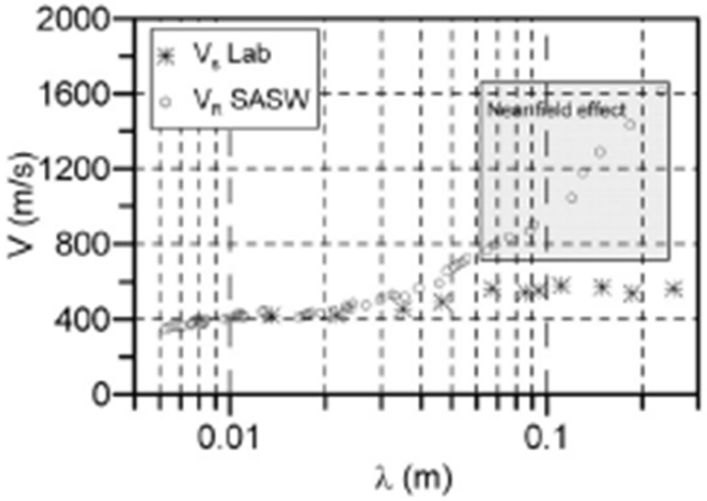

Figure 2- 15 Comparison of shear wave velocities obtained from the centrifuge and laboratory test for Model B (B6) (Murillo et al., 2009)

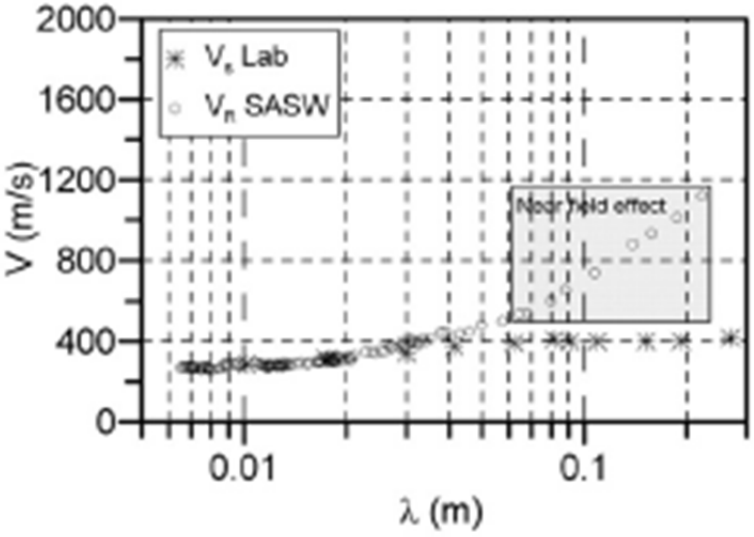

Figure 2- 16 Comparison of shear wave velocities obtained from the centrifuge and laboratory test for Model C (A3) (Murillo et al., 2009)

Thus Murillo et al. (2009) concluded by stating that the shear wave velocity values obtained on the homogeneous models, using the conventional technique, satisfactorily agreed with the results obtained from the laboratory tests. But for higher depths, the results obtained using the SASW method were affected by the near field effect, and, therefore, showed a large discrepancy with the laboratory tests.

2.5 Summary

The Spectral Analysis of Surface Waves method is a non-intrusive method which uses Rayleigh wave measurements in the field to calculate the shear wave velocity profile of geotechnical sites. The shear wave velocity profiles give a thorough picture of the ground profile at the site. Also, in comparison to other borehole methods, SASW proved to be more accurate, fast and cost-effective.

This chapter dealt with an introduction, history and development of the seismic geophysical tests, an overview of wave propagation and the various in-situ tests implemented over the years. A few seismic non-intrusive tests were also briefly discussed. The following chapters will deal with the test procedure, analysis and results.

Chapter 3

Experimental Program

3.1 Introduction

The experimental program for the current research involves basic soil characterization and assessment of strength improvement. This chapter contains the procedural details and fundamental test results pertaining to the Controlled Low Strength Material (CLSM) mix. The UCS and Resonant Column test procedures are presented in this chapter. The test procedure for the Spectral Analysis of Surface Wave (SASW) method has been elucidated. In addition, apparatus details employed in the SASW test are also stated. Figure 3-1 depicts the experimental program in the form of a flowchart.

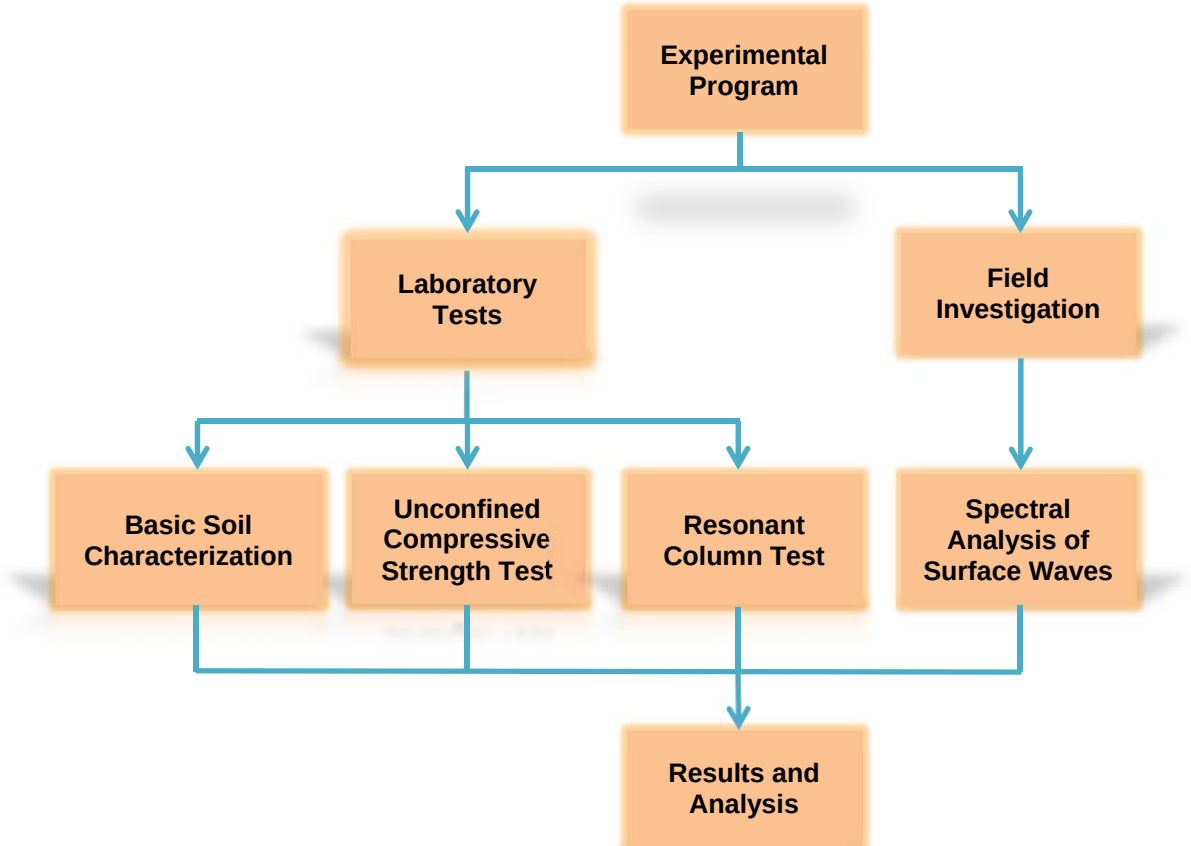

Figure 3-1 Flowchart representing the tests conducted in the Experimental Program

3.2 Laboratory Tests

Basic soil characterization, the UCS test and the Resonant Column test form the bulk of the laboratory testing in the current research.

3.2.1 Basic Soil Characterization

The soil used in this research was collected in Mansfield, Texas. It was a mixture of the native soil, cement and water, i.e., CLSM (Controlled Low Strength Material). The coarse sand had a coefficient of curvature (C_c) of 4.8 and a coefficient of uniformity (C_u) of 71.4. Further, the following tests were conducted to determine the CLSM properties.

3.2.1.1 Particle Size Analysis

Particle size analysis includes a sieve analysis and hydrometer analysis in accordance with the ASTM D 422 standard. First, the CLSM was crushed to perform the sieve analysis to determine the percentage of soil retained on the No.200 sieve. Then, the soil passing through No.200 sieve was used to perform the hydrometer test to determine the percentage of finer soil corresponding to the particle size. Both of these tests are demonstrated as a particle size distribution curve in Figure 3-2.

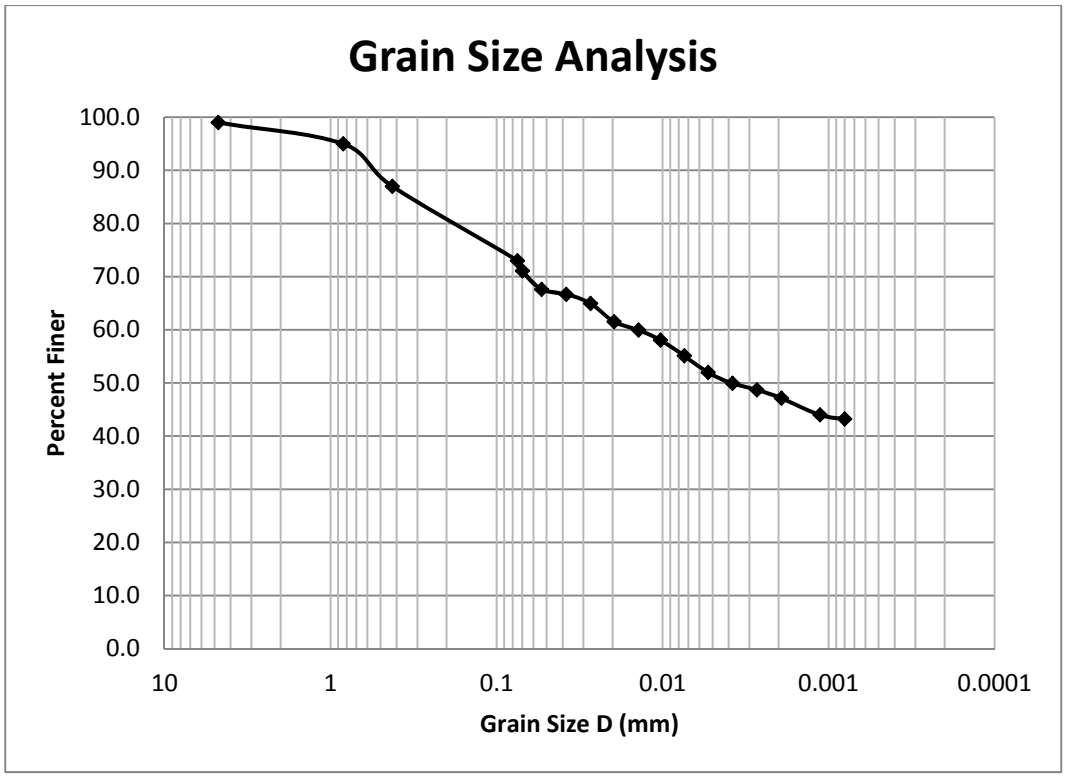

Figure 3- 2 Particle Size Distribution Curve

3.2.1.2 Atterberg Limits

Atterberg limits define the state of the soil based on its moisture content. In the current research, liquid limit and plastic limit of the soil were determined in accordance with the ASTM D 4318 standard. The moisture content at which the soil passes from a liquid state to a plastic state is termed as liquid limit. Similarly, the moisture content at which the soil transforms into a semi-solid state from a plastic state is termed as plastic limit. In addition, shrinkage limit is defined as the moisture content at which the soil changes from a semi-solid state to a solid state. The values of liquid limit and plastic limit of the CLSM are presented in Table 3-1.

Table 3- 1 Physical Properties of CLSM

Basic Soil Properties	
Percent Passing No. 200 Sieve	73
USCS Classification	CL
Liquid Limit, LL	24.39
Plastic Limit, PL	14.29
Plasticity Index, PI	10.1
Specific Gravity, G_s	2.62

3.2.1.3 Specific Gravity

The specific gravity of a given material may be defined as the ratio of the density of a given volume of the material to the density of an equal volume of water. Specific gravity is denoted by G_s. The specific gravity test was conducted in accordance with the ASTM D 854 standard. The value of G_s of CLSM is also presented in Table 3-1.

3.2.2 Unconfined Compressive Strength (UCS) Test

The Unconfined Compressive Strength (UCS) test was performed in accordance with the ASTM D 2166 standard. The primary objective of the UCS test is to determine a compressive strength for soils which possesses ideal cohesion to enhance testing in the unconfined state. The test procedure was initiated by placing the soil sample on the loading platform. A top cap was placed on top of the sample. The loading platform was raised slowly, until the top cap on the soil specimen touched the top plate of the triaxial setup. An external LVDT (Linear Variable Displacement Transducer) was connected so that its tip touched the top portion of the top plate of the triaxial setup. Once the setup was ready, the test progressed by inducing a lift to the soil specimen at a constant rate. As the specimen was raised, the

LVDT measured the displacement, while the load cell measured the applied load. The test was stopped when the sample started to show signs of cracking. The load required to cause the sample to fail was noted and the axial stress was thus calculated. The maximum axial stress obtained was the unconfined compressive strength of the soil. Figure 3-3 illustrates the equipment employed in this research to perform the unconfined compression test.

Figure 3- 3 Test set-up for UCS test

3.2.3 Resonant Column Test

The Resonant Column (RC) testing technique was first used to study the dynamic properties of rock materials in the early 1930s, and has been continuously evolving since then for the dynamic characterization of a wide variety of geologic materials (Huoo-Ni, 1987).

The Resonant Column test is used to determine the shear modulus and damping properties of soils. In the current research, it was performed in accordance with the ASTM D 4015 standard. Figure 3-4 illustrates a summary of the test procedure for the Resonant Column test implemented in this research. The test essentially consists of a cylindrical soil specimen confined between two ends. The bottom end is usually fixed, while the top end is capable of exciting the specimen by inducing torsional or longitudinal vibrations. An open-top chamber of water surrounds the specimen to provide uniform confinement. The top cap, connected to a circuit, is then placed over the top of the specimen to induce torsional vibrations in the specimen. A solid metal chamber is then placed over the soil specimen surrounded by the water chamber to maintain the air pressure inside the setup.

The operation of the Resonant Column test has been mentioned in brief previously. A vibration is applied using an electromagnetic drive system with variable frequency at the top of the sample, with the bottom held in place. This results in a frequency response curve. Once the frequency at resonance is experimentally known, the shear wave velocity and, hence, the shear modulus of the soil can be determined. According to Richard (1975), the frequency curve can be used to derive a small strain shear modulus (G) as follows:

$$G = \rho\,(2\pi L)^2 \left(\frac{f_r}{F_r}\right)^2 \tag{3.1}$$

$$F_r = \sqrt{\frac{I_R}{I_o}} \tag{3.2}$$

where ρ = soil density, L = sample length, f_r = resonant frequency, F_r = driver constant, I_R and I_o are polar moment of inertia of soil column and driver system, respectively.

a) Initial placement of the Soil Specimen

b) Placement of the water chamber

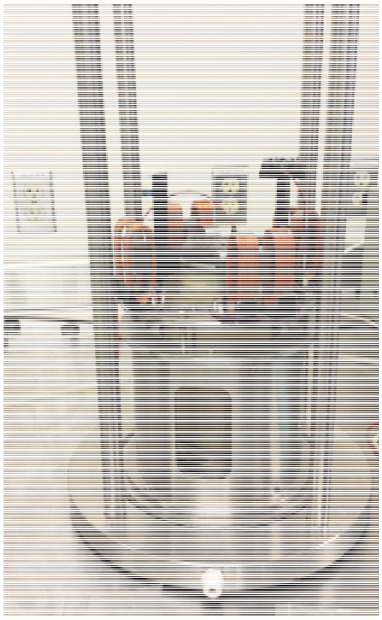

c) Placement of Electromagnetic Drive System

d) Final Setup

Figure 3- 4 Resonant Column Test Procedure

3.3 Field Test

The field testing in this research was mainly focused on determining the stiffness of CLSM by improvising the Spectral Analysis of Surface Wave (SASW) method, (a non-destructive technique). The test site is a part of the Integrated Pipeline (IPL) project running along the J1 line, located in Mansfield, Texas. The SASW tests were performed in a prove-out section of the pipeline, which measured a length of 500 feet. Figures showing the test site section with the pipe and the pouring of CLSM are presented below.

Figure 3- 5 Installation of the Pipeline in the Prove-out Section

Figure 3- 6 CLSM around the Pipeline in the Prove-out Section

Figure 3- 7 Testings inside the Pipeline

3.3.1 Spectral Analysis of Surface Wave (SASW) Method

The apparatus employed to perform the spectral analysis of the surface wave method, in this research, is illustrated in Figure 3-8. The apparatus mainly consists of four components. They are: 1. Impact Source (hammer), 2. Receivers, 3. Connecting wires and 4. Data Logger.

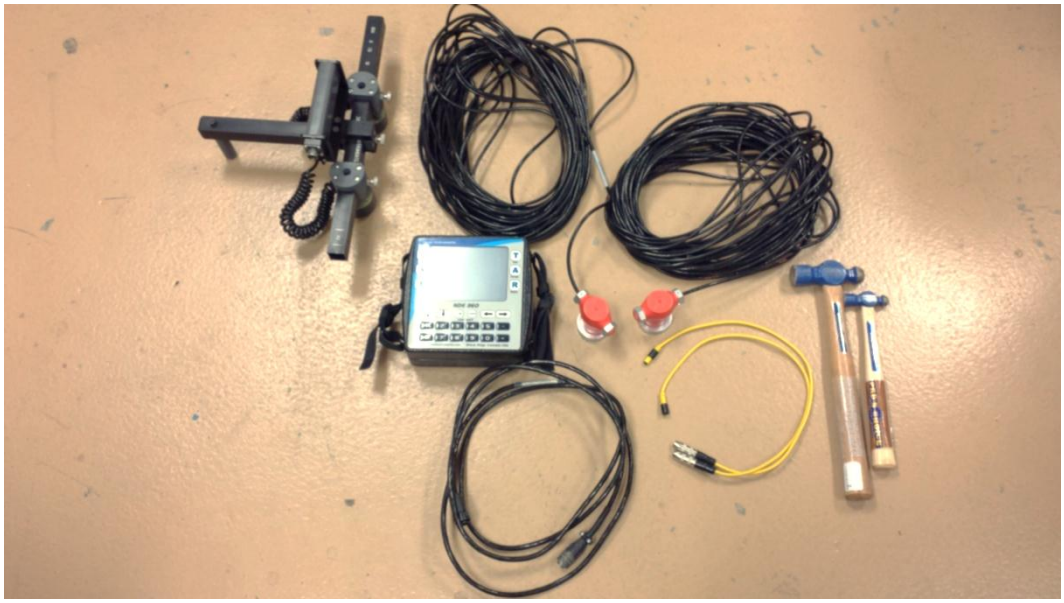

Figure 3- 8 SASW Test Apparatus

3.3.1.1 Impact Source

In the current research, hammers were used as impact sources. Hammers were chosen in accordance with the necessary depth of investigation. Smaller hammers generate high frequency waves, while larger hammers generate low frequency waves. In the case of the lower depths of investigations, smaller hammers are preferable owing to their generation of high waves, i.e., low wavelengths. On the contrary, larger hammers are preferred for greater depths of investigations owing to their generation of low frequency waves, i.e., higher wavelengths. SASW tests were performed in a 1.5 inch thick steel pipeline. The depth of

investigation was not more than 3 feet. Thus, a 4 ounce hammer was improvised. Figure 3-9 illustrates the various hammers available.

Figure 3- 9 Various Hammers used to provide Impact

3.3.1.2 Receivers

The SASW equipment consisted of two types of receivers. First, a pair of displacement transducers was connected in line with a bar. This was used to perform SASW tests on hard surfaces. Second, a pair of geophones, with a frequency of 1 hertz, was used with a flat receiver base. Provision was also given for a spiked receiver surface in the case of very loose soil. These geophones were implemented to perform SASW tests on soil. Figure 3-10 illustrates both of the types of receivers.

Figure 3- 10 Displacement Transducer (Above) and Geophones (Below)

3.3.1.3 Connecting Wires

Connecting wires, commonly known as cables, were used to connect the receivers to the data logger. Figure 3-11 shows a picture of these cables.

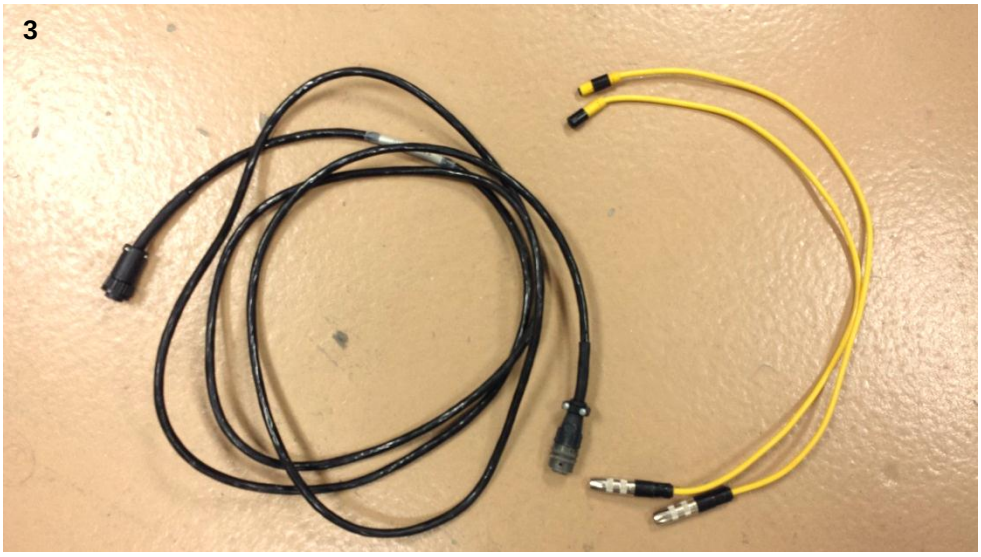

Figure 3- 11 Connecting Cables

3.3.1.4 Data Logger

Olson Instruments provided a data logger to monitor the performance and the efficiency of the SASW tests. In the current research, this data logger is more commonly known as NDE 360. The NDE 360 is connected to the receivers by cables. When the settings are customed accordingly, the NDE 360 displays the phase velocity and the coherence of the waves generated in the presence of an impact. This facilitates identifying the efficiency of the wave and thus deducing the subsurface material properties. Figure 3-12 illustrates the NDE 360.

Figure 3- 12 Data Logger (NDE 360)

3.3.1.5 Sasw Method - Test Procedure

The SASW test procedure is initiated by selecting the type of receiver to be used in accordance with the surface to be tested. In the current research, the surface to be tested was a solid surface (pipeline); thus, the displacement transducer was selected. The depth of the investigation was 4 feet; therefore, a spacing of 2 feet was provided between the two receivers. This was performed in accordance with the Olson manual, which states that the distance between the two receivers is supposed to be half the desired depth of investigation. Once the receivers were selected, they were connected to the NDE 360 (Data Logger) by connecting cables. Impact points were selected at a distance of 2 feet (equal to the receiver spacing) from either receiver. The NDE 360 was then switched on and the necessary settings were performed. The settings included the following:

- The gain for both the channels was made equal to 100.
- The parameter settings were performed by pressing the “Param” knob.
- Time/pt. (us) was set to a value of 200.
- Spacing was provided in inches.
- The trigger channel and the reference channel were selected based on forward or reverse direction of the test.
- Finally the name of the file to store the data was created.

The above was followed by providing an impact at the impact point to generate surface waves. These surface waves were recorded by the receivers. The phase difference and coherence of the wave are displayed in the NDE 360. The data was then stored and analyzed for results.

3.4 Summary

This chapter presents the fundamental laboratory tests and their results. Test soil from the field is characterized based on the laboratory tests. The test procedures for the UCS and the Resonant Column test have been discussed step-by-step in accordance with the ASTM D 2166 and ASTM D 4015 standards, respectively. A brief overview of the proveout section used to assess the quality of bedding CLSM material is discussed in this chapter. The SASW test procedure and the apparatus employed in performing the tests have been discussed, with the help of illustrations.

Chapter 4

Laboratory Investigations

4.1 Introduction

The results obtained from the laboratory investigations are analyzed and presented in this chapter. Unconfined Compressive strength (UCS) test results were utilized to study the strength gain in CLSM with time. Similarly, resonant column test was utilized to study the stiffness gain in CLSM with time. This chapter details the strength and stiffness test results obtained from laboratory investigations.

4.2 Unconfined Compressive Strength Test

The objective behind performing the UCS tests was to determine the increase in the stiffness of CLSM over time. UCS tests were conducted on field cast samples after 1, 3, 7, 14 and 28 days. The samples were collected from the field in molds. The dimensions of the collected samples were 6 inches in diameter and 12 inches in height. TRWD made different trial mixes of CLSM before finalizing the percentage of cement to be used in the preparation of CLSM. The trial mixes were prepared using 4%, 6%, 8% and 10% of cement in the field (Raavi, 2012). Implementation of 4% of cement also proved to be cost-effective when compared to the other trial mixes. Hence, the final mix design of CLSM consisted of 4% of cement. The unconfined compression tests were conducted in accordance with the ASTM D 2166 standard. Table 4-1 provides a summary of the UCS test results over time. Figure 4-1 illustrates a plot to describe the UCS test results with respect to time.

Table 4- 1 Summary of UCS Test Results

Time	Unconfined Compressive Strength							
	Sample 1		Sample 2		Average		Standard Deviation	
	kPa	psi	kPa	psi	kPa	psi	kPa	psi
Day 1	38	5.5	41.9	6	39.9	5.8	2.0	0.3
Day 3	101.3	14.7	92.3	13.4	96.8	14.1	4.5	0.6
Day 7	432.7	62.7	468.1	67.9	450.4	65.3	17.7	2.6
Day 14	858.3	124.5	1001.1	145.2	929.7	134.9	71.4	10.4
Day 28	1027.3	149	1048	152	1037.6	150.5	10.4	1.5

Tarrant Regional Water District (TRWD) recommended a CLSM strength ranging between 70 and 150 psi after 28 days of casting for the current research. Also, through Figure 4-1, it can be observed that there is a strength increase of CLSM evident with time. From the chart, it can be observed that the TRWD recommended design strength is achieved by the CLSM after 7 days of cast.

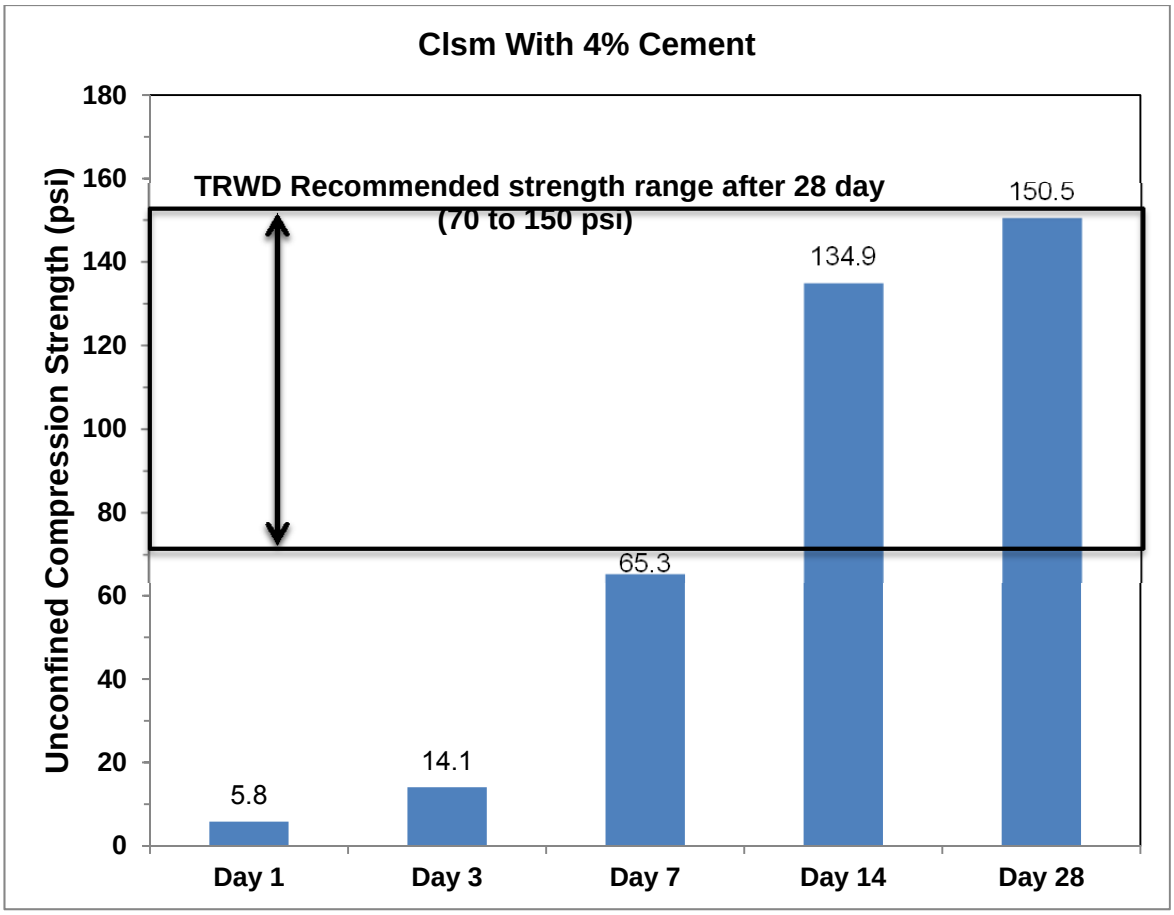

Figure 4- 1 Graphical representation of UCS Test Results with Time

4.3 Resonant Column Test

In the laboratory. 4% cement was employed in preparing the samples, and each sample had a diameter of 2.8 inches and a height of 5.6 inches. Replicate samples were prepared with respect to time, i.e., days 1, 3, 7 and 14 and then tested for stiffness using resonant column apparatus. Frequency response curves of the soil specimens cast at different days are presented in Figures 4-2 to 4-5. Figure 4-6 illustrates the frequency response curves of replicate samples after 14 days of curing. The difference in the peak values observed in replicate studies is minimal. Thus an average value of the two samples for each day has been

considered. The results obtained are summarized in Table 4-2. Figure 4-7 illustrates a summary of the frequency response curves obtained from the Resonant Column test. Figure 4-8 presents the variation of shear modulus (calculated from the Resonant Column test) with time. A comparison of these results with the field results is illustrated later in this chapter.

Table 4- 2 Resonant Column Test Results

Time (days)	**Confining Pressure (psi)**	**Input Voltage (V)**	**V_{rms} at f_r (V)**	**0.707*V_{rms} (V)**	**f_r (Hz)**	**Shear Modulus, G (MPa)**	**V_s (m/s)**
1	15	0.25	0.1040	0.0735	146.7	200.5	333.7
3	15	0.25	0.2131	0.1507	157.4	230.7	357.9
7	15	0.25	0.2247	0.1589	167.2	260.3	380.1
14	15	0.25	0.2043	0.1444	179.5	300.3	408.3

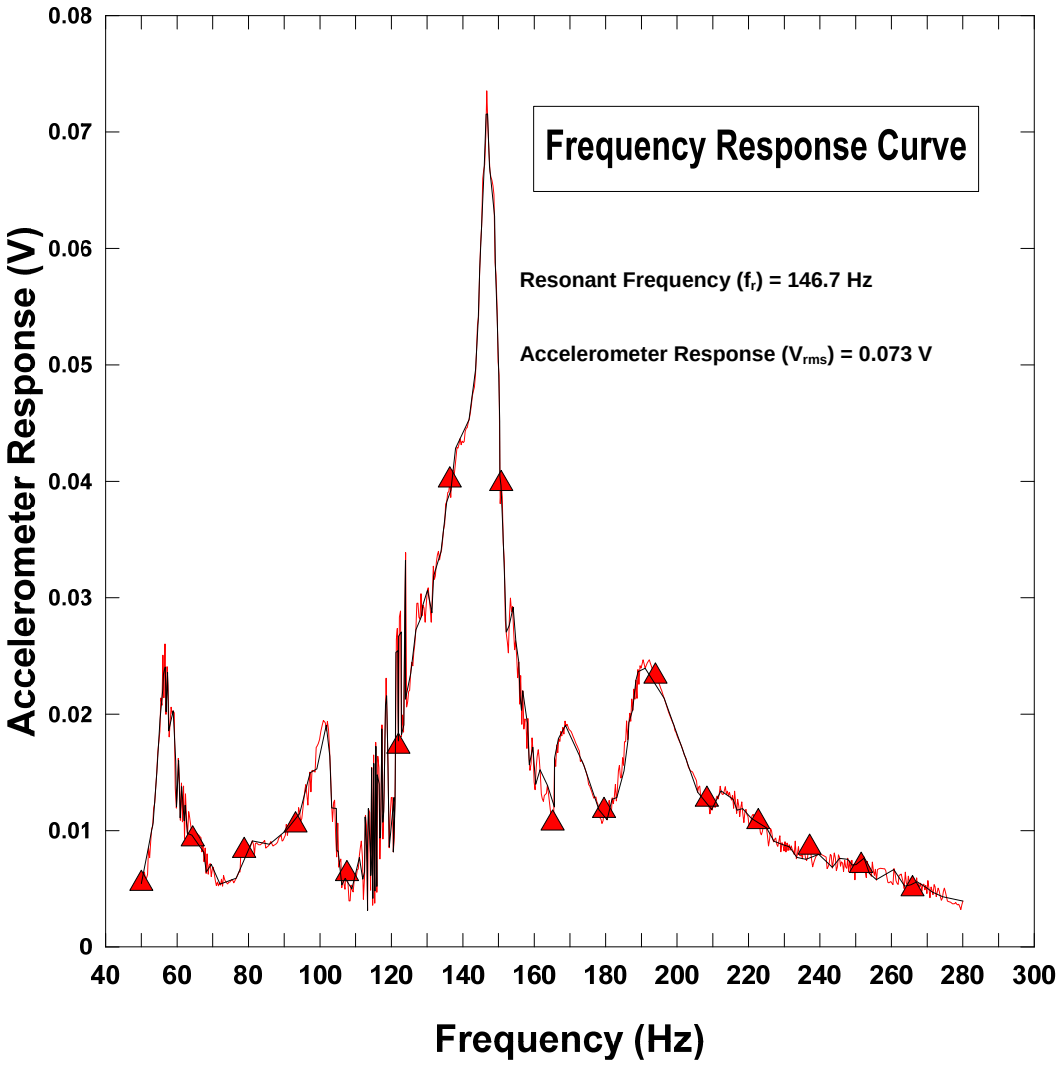

Figure 4- 2 Frequency Response Curve for Day 1

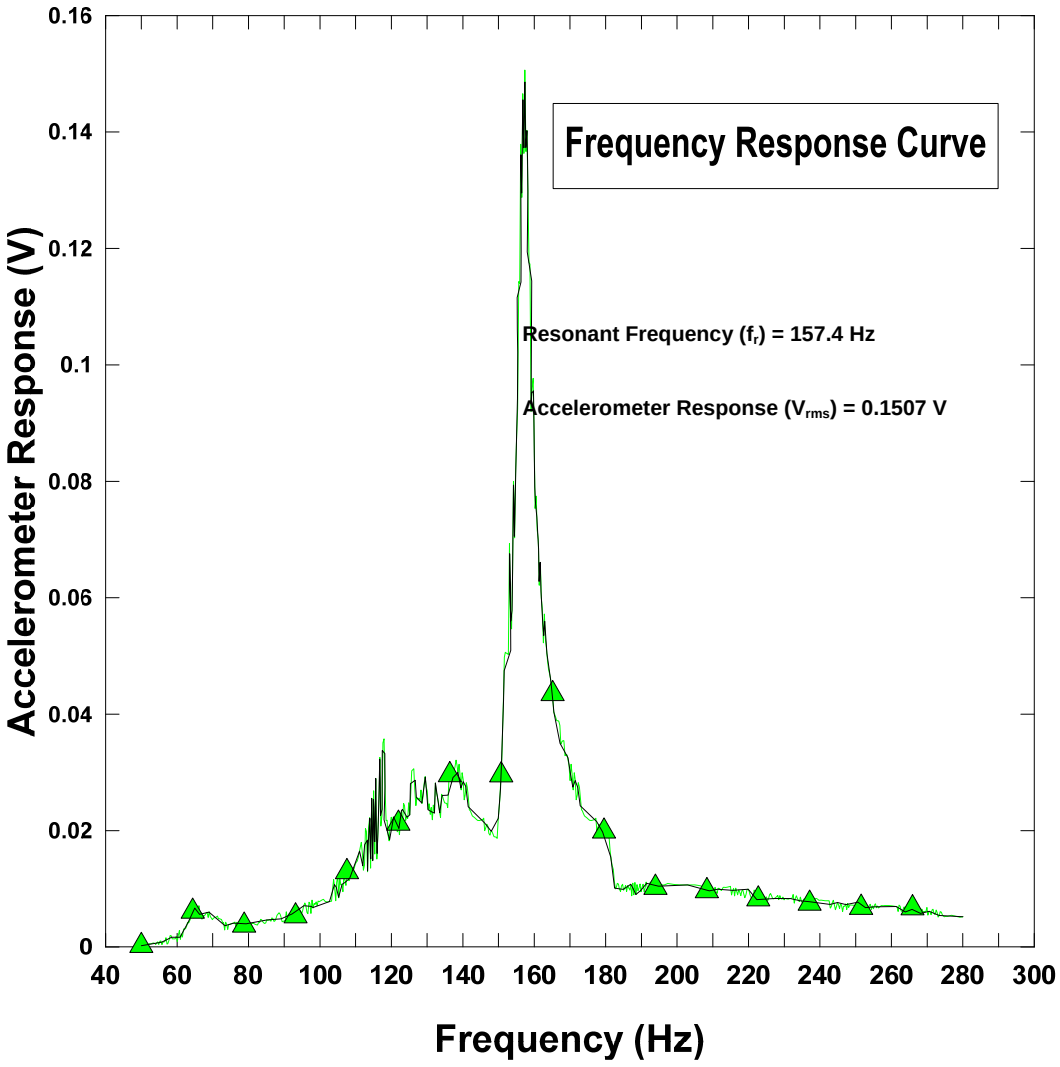

Figure 4- 3 Frequency Response Curve for Day 3

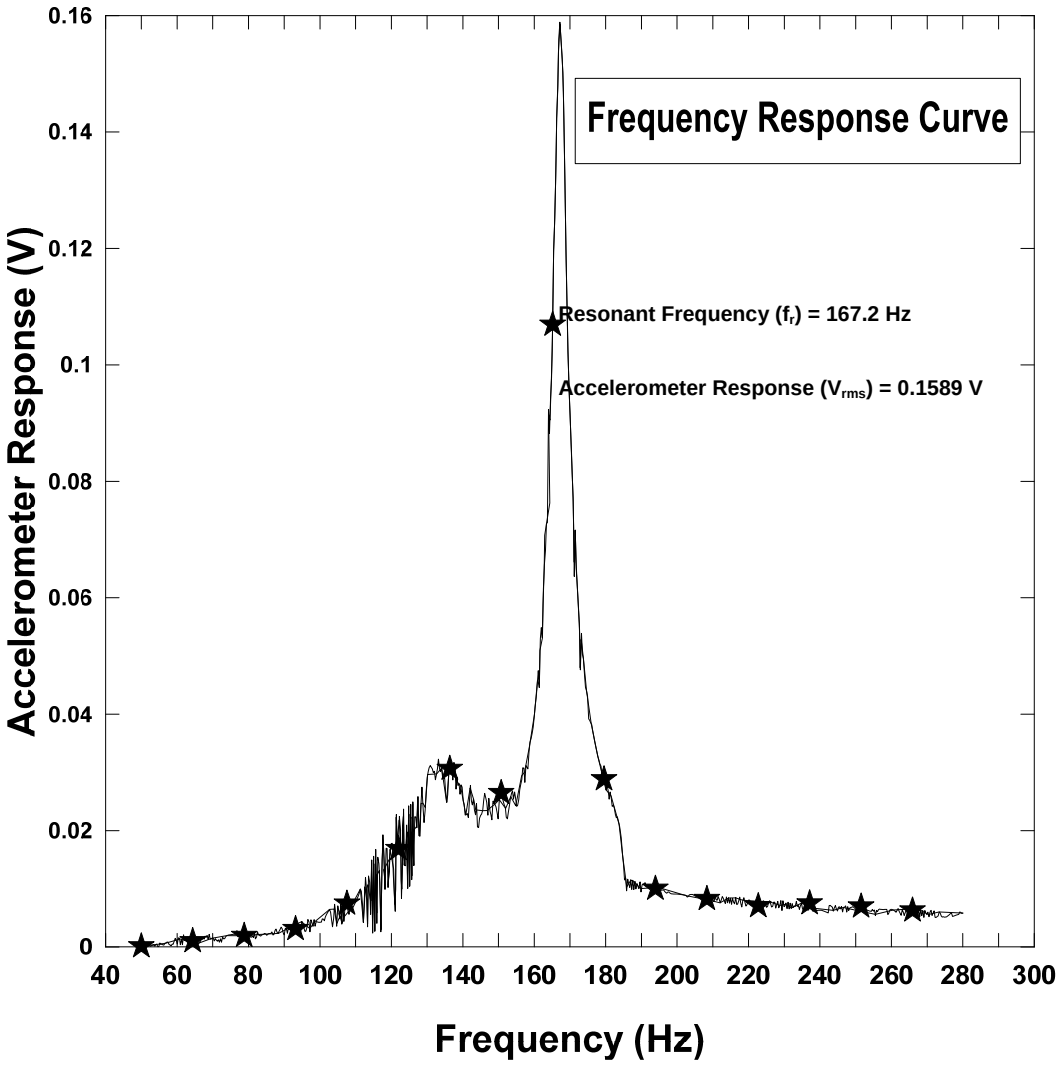

Figure 4- 4 Frequency Response Curve for Day 7

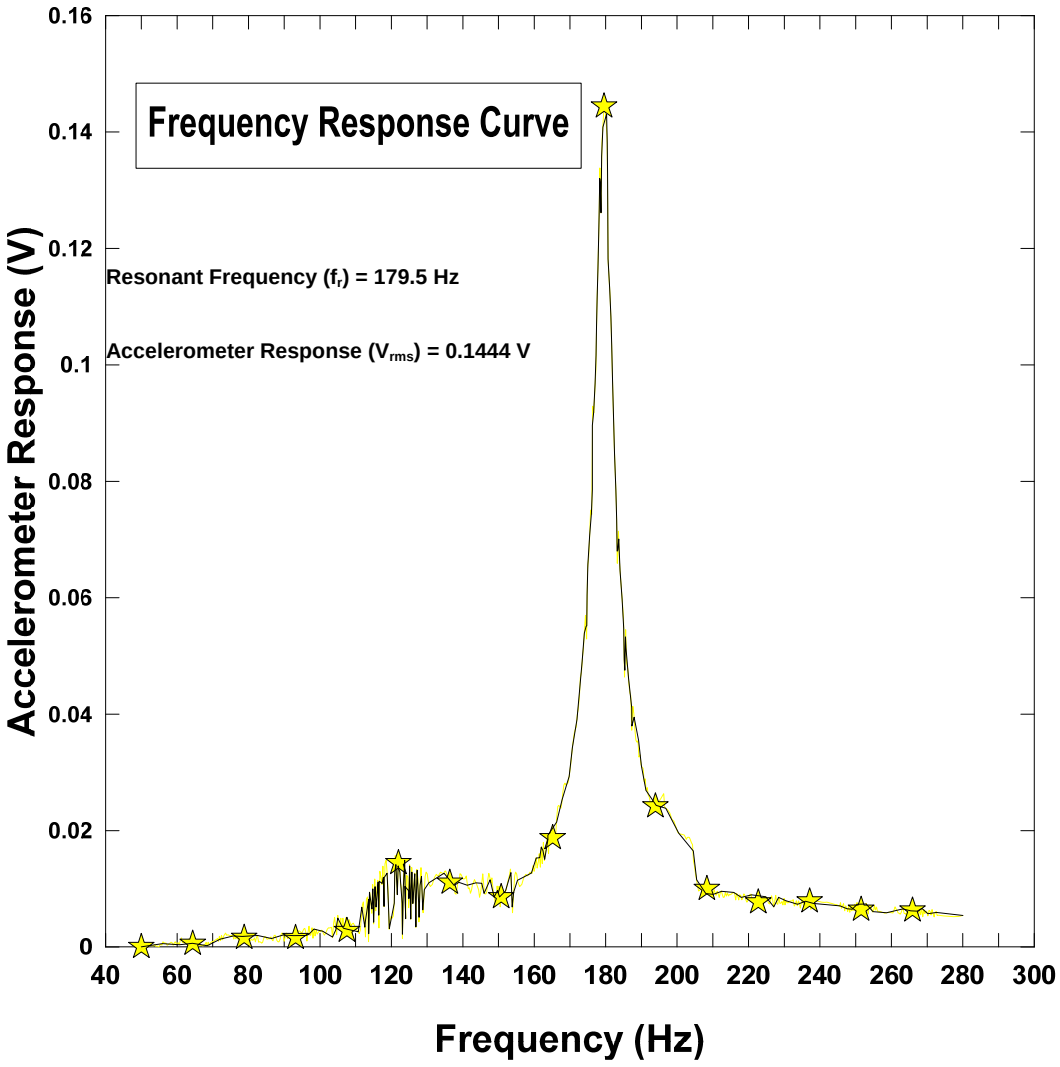

Figure 4- 5 Frequency Response Curve for Day 14

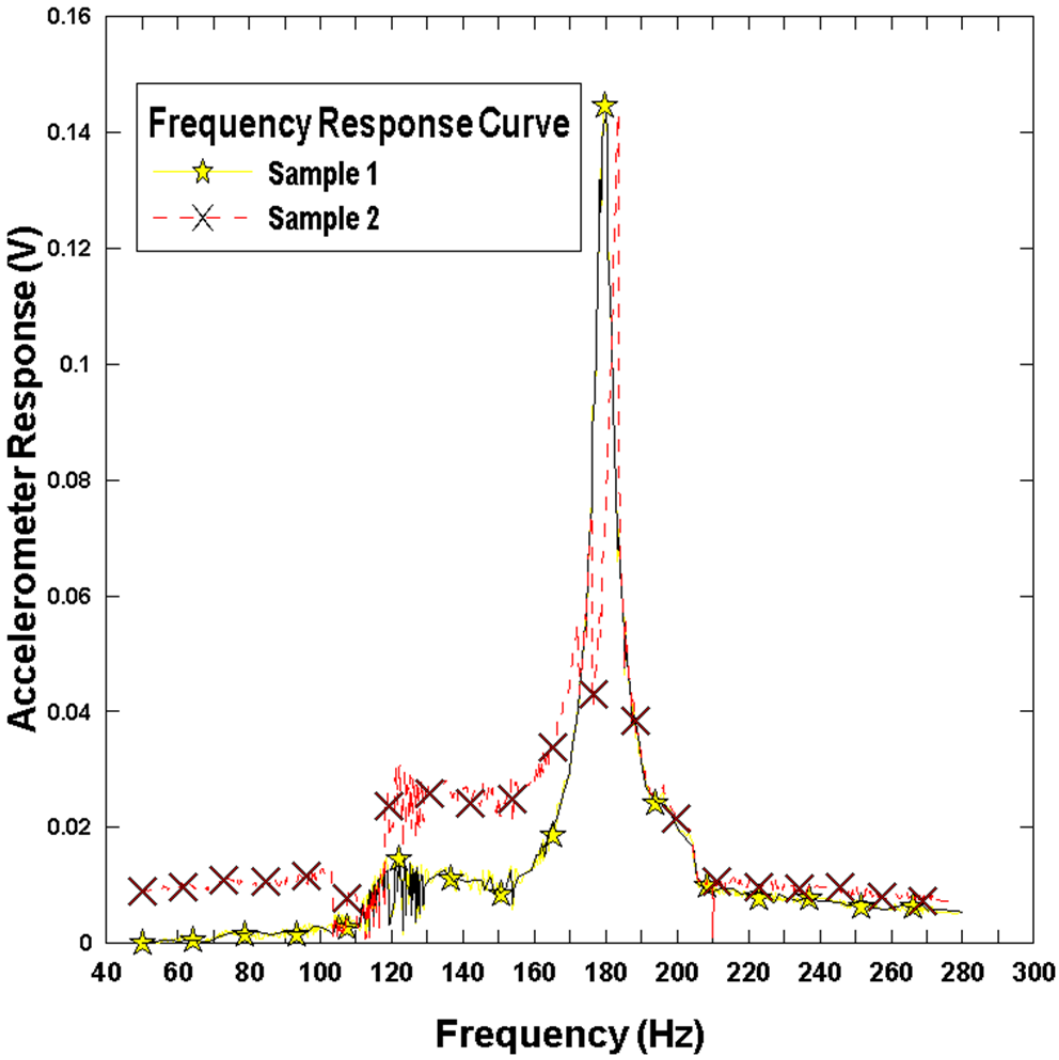

Figure 4- 6 Frequency Response Curves of Two Samples for 14 days curing

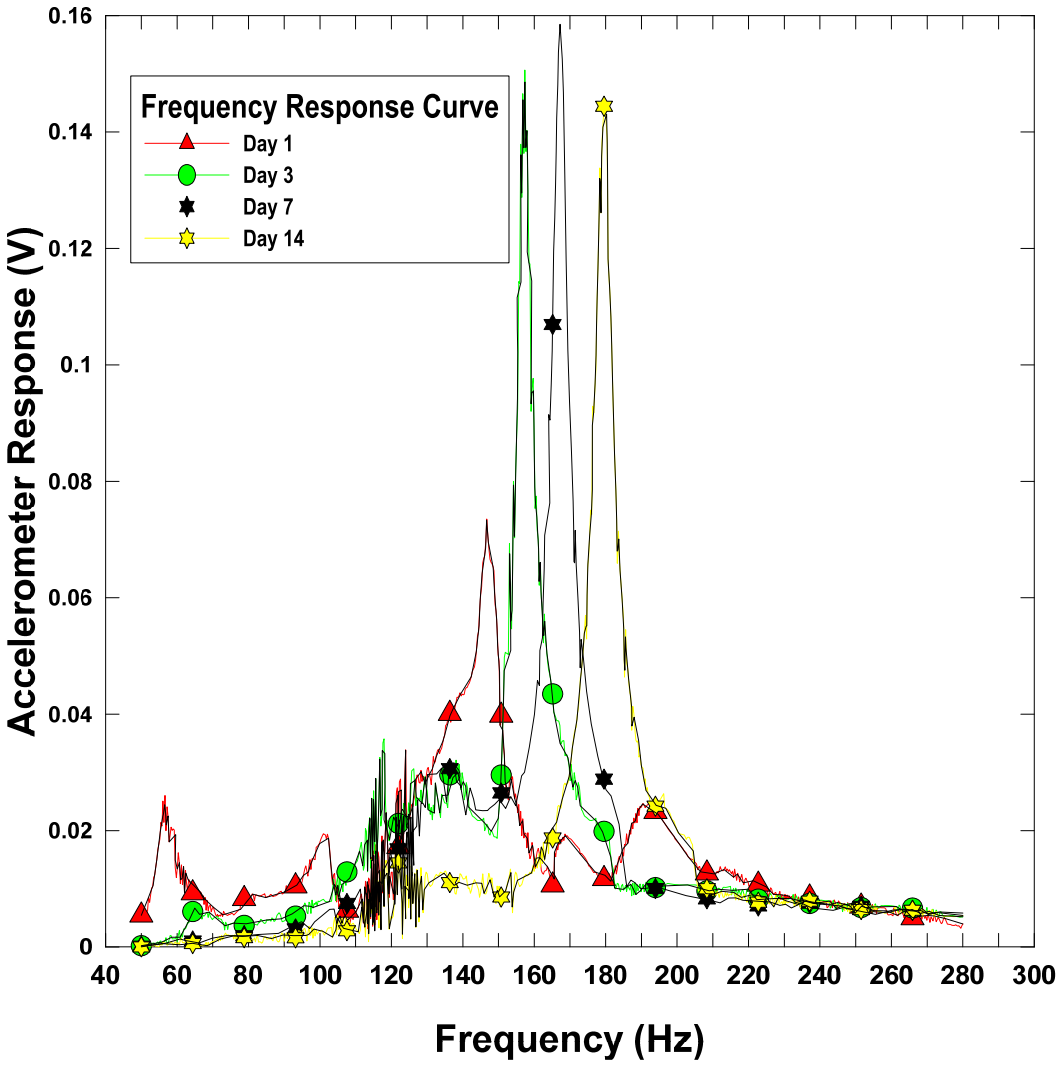

Figure 4- 7 Summary of frequency response curves for Days 1, 3, 7 and 14

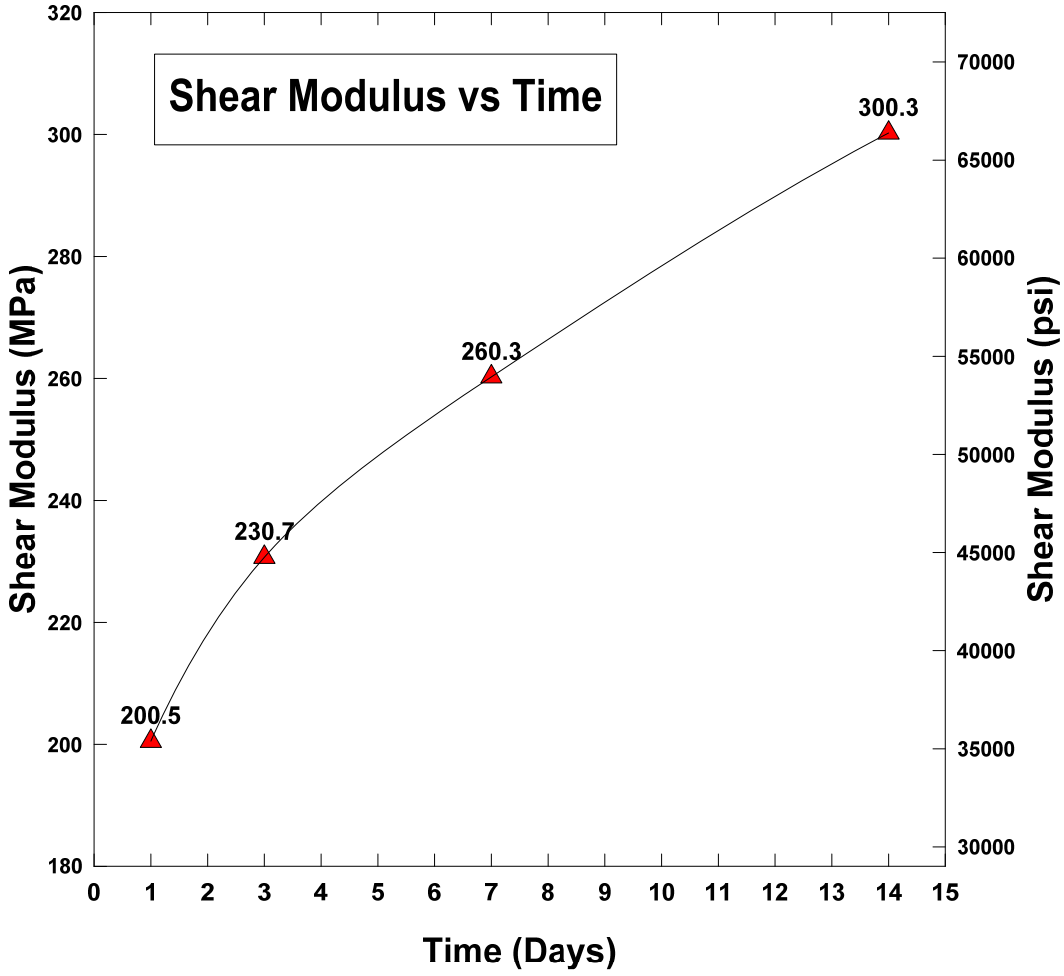

Figure 4- 8 Variation of Shear Modulus with Time for RC Test

4.4 Summary

This chapter presents the laboratory test investigations. The results of the UCS test showed that the obtained results from CLSM are in compliance with the TRWD recommendations. The Resonant Column test results have been conducted using standard testing procedure. Field investigation studies conducted by SASW test results and analysis are presented in Chapter 5.

Chapter 5

Field Test Investigations

5.1 Spectral Analysis of Surface Waves

The spectral analysis of the Surface Wave method (SASW) was performed inside a pipeline as illustrated in Chapter 3. Seventeen (17) test sections were selected along the prove-out section of the pipeline. The prove-out section extended to a length of 500 feet. Five (5) points (South 2, South 1, Center, North 1, and North 2) were selected at each section to determine the variation in stiffness of CLSM across the pip of each section. . Figure 5-1 illustrates the 17 test sections selected, and Figure 5-2 depicts the cross-section of the pipe defining the alignment of test points at each section and the procedure followed to conduct the field investigations. Sections 1070-50 and 1071-50 represent joints in the pipeline. Besides in pipe testing, SASW tests were performed at joints to determine the variations of stiffness of CLSM in comparison to the stiffness of CLSM at the other sections.

As mentioned in the experimental program, SASW tests were performed with a geophone spacing of 2 feet. A geophone spacing of 2 feet yields shear wave velocity measurements up to a depth of 4 feet.

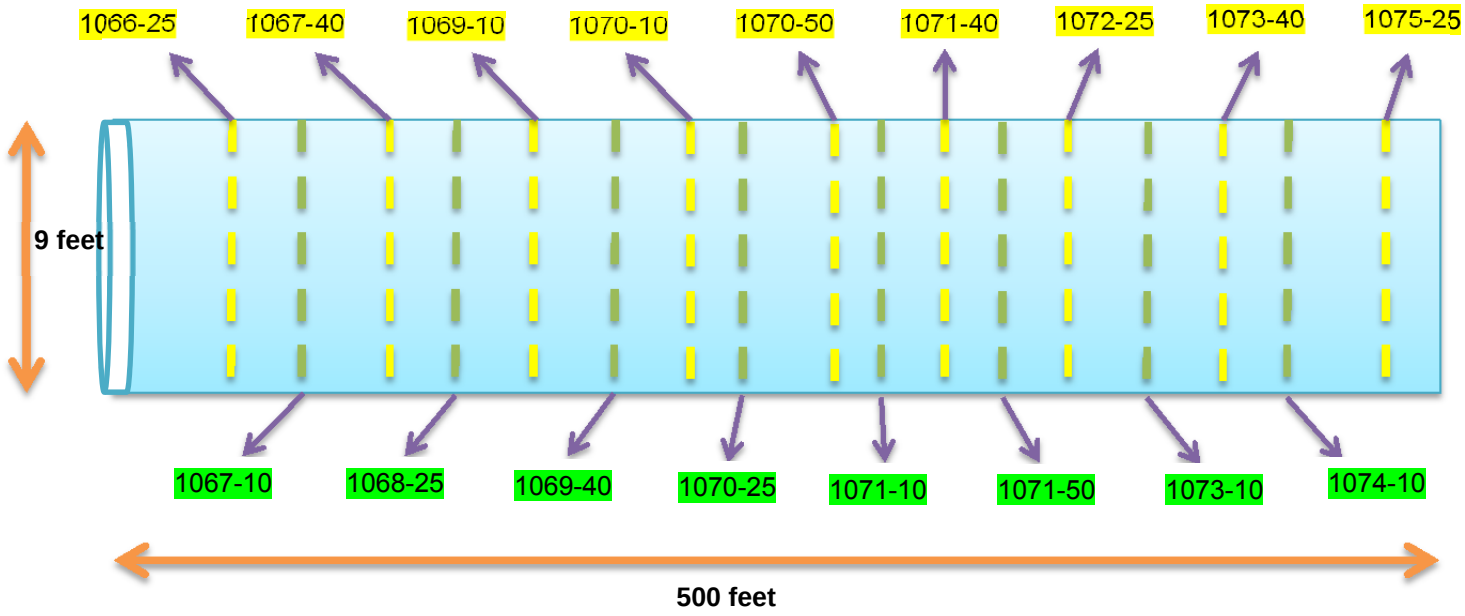

Figure 5- 1 The 17 test sections selected inside the pipe

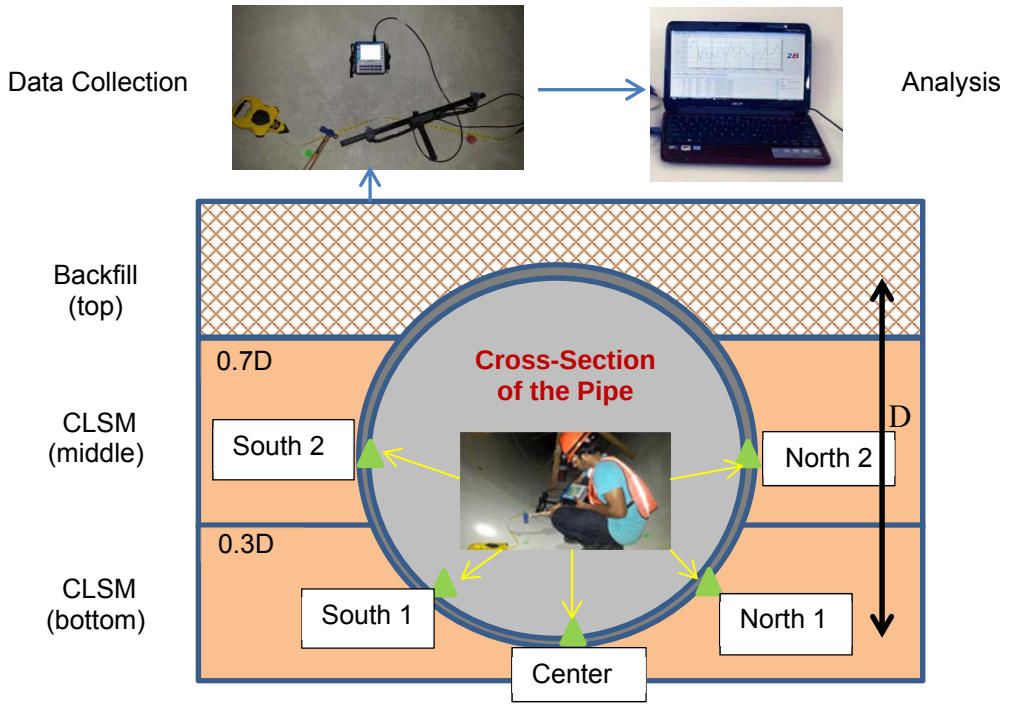

Figure 5- 2 Cross-Section of the pipe displaying the 5 test points and the SASW test procedure

The procedure to conduct the SASW is detailed in Chapter 3. The data acquisition and data analysis were accomplished by employing WinTFS and WinSASW software, respectively. The procedures implemented to conduct data analysis, using the above mentioned software, have been detailed henceforth.

5.2 Analysis of SASW Data

5.2.1 WinTFS

The data acquired from the SASW tests was stored by the NDE 360 (data logger) in the ".nde" format. The analysis by WinTFS was initiated by importing, the

SASW data. The data was windowed to eliminate the undesired non-surface wave. As suggested by Olson Instruments, Inc., a decay factor of 3500 was employed in windowing the data. Windowing was followed by masking the data. Masking was performed to avoid unwanted disturbances in the data caused by any movements in the surrounding area while conducting the SASW test. This measure enhanced the accuracy of the results. The SASW test properties employed included transducer spacing of 2 feet (0.6096 meter), Poisson's ratio of 0.2 and mass density value of 1800 kg/m^3. With the input of these properties, WinTFS yielded a dispersion curve (a plot between surface wave velocity and wavelength). Figures 5-3 to 5-6 illustrate the stepwise procedure employed in the analysis by WinTFS.

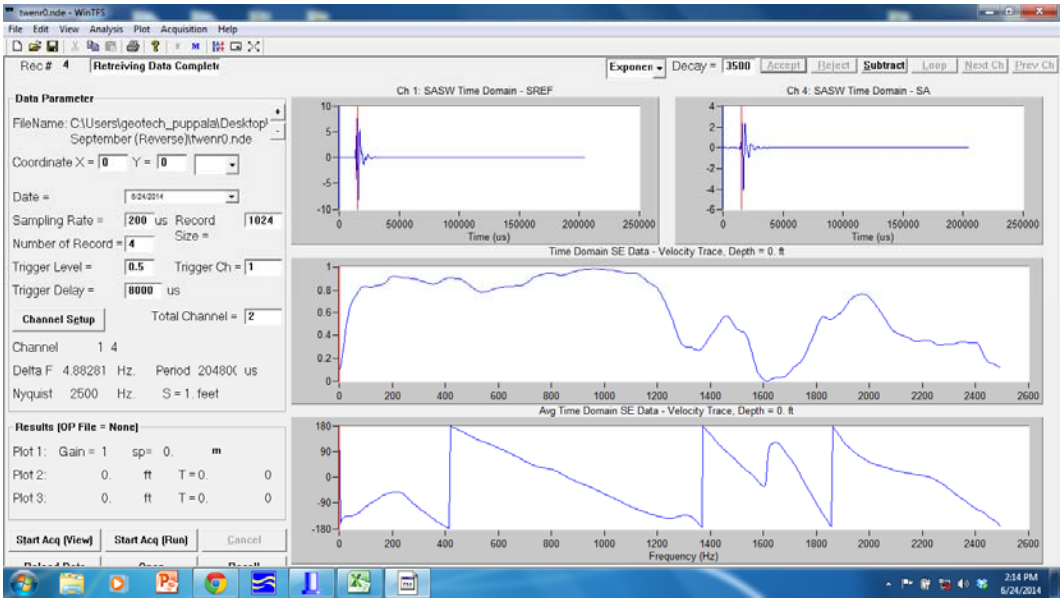

Figure 5- 3 Initial import of the SASW data

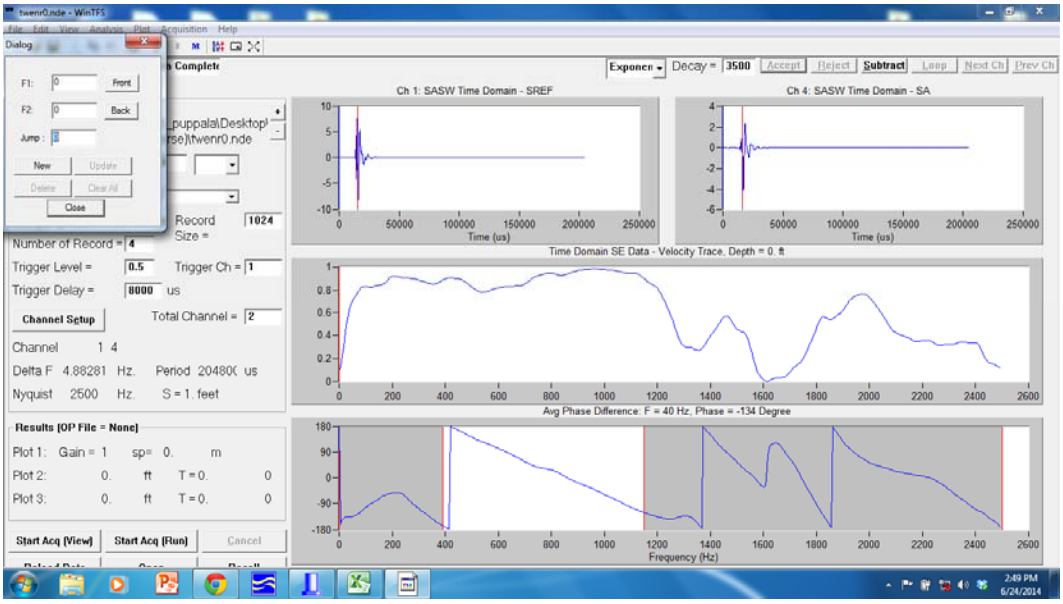

Figure 5- 4 Masking the SASW data

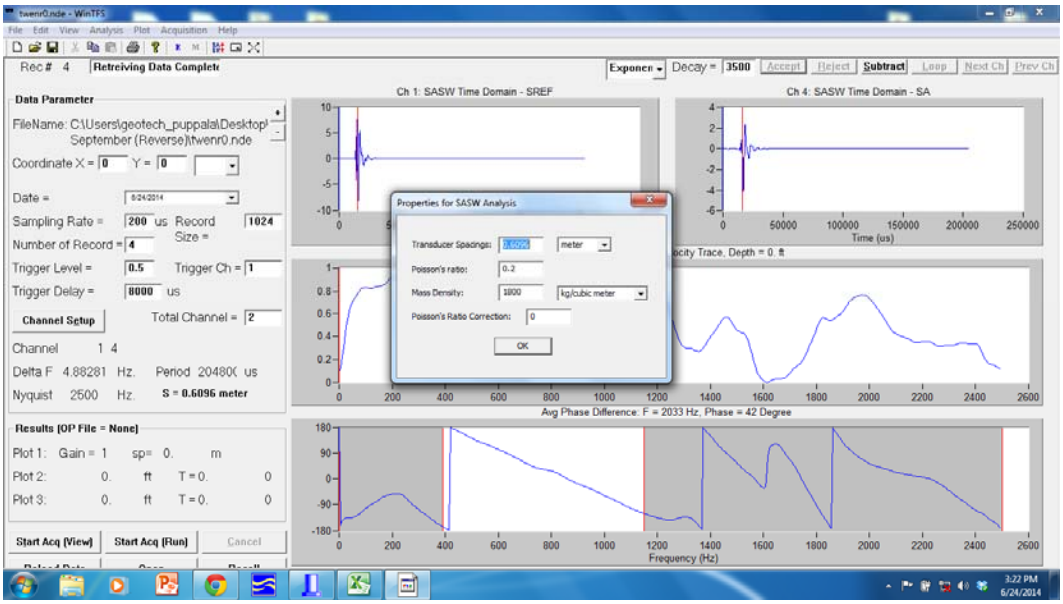

Figure 5- 5 Validation of SASW properties

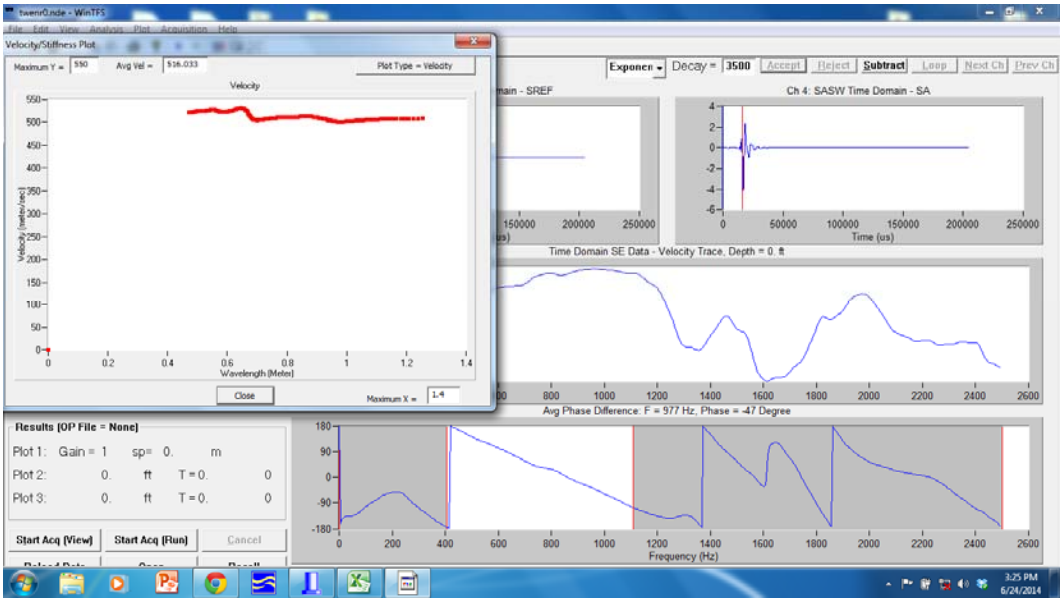

Figure 5- 6 Final Dispersion Curve

The dispersion curve indicated an average value of the shear wave velocity of the CLSM layer and the underlying soil layers.. Also, the data analyzed through WinTFS yielded data files of various other formats such as “.coh”, “.msk” and “.hyx”. The data file of “.hyx” format was employed in analyzing the data through WinSASW software in order to generate a depth-wise profile of the subsurface.

5.2.2 WinSASW

The analysis by WinSASW was performed with the main objective of distinguishing the CLSM layer from the other subsurface soil layers. WinSASW results implicated the variation of shear wave velocity with respect to depth in the CLSM-soil profile. This aided in distinguishing CLSM from the other layers and also enabled the interpretation of the thickness of each layer. Analysis by WinSASW was initiated by importing and loading the data with the inputs of the necessary source and receivers locations. This was succeeded by the process of masking the data to eliminate any undesirable disturbances present in the data. The dispersion curve, which implies to the experimental curve, was then generated.

A theoretical curve, to match the experimental curve, was then generated by assuming the various necessary parameters by a trial and error approach. These parameters included thickness, shear wave velocity, density, Poisson's ratio and damping factor for the assumed number of layers. After many trial and error tests, the assumed values of each of the above mentioned parameters were attained and are illustrated in Figure 5-11. Once the theoretical curve was matched with the experimental curve, the results obtained enabled the determination of the variation of shear wave velocity with respect to depth. Figures 5-8 to 5-12 illustrate the stepwise procedure employed in the analysis by WinSASW.

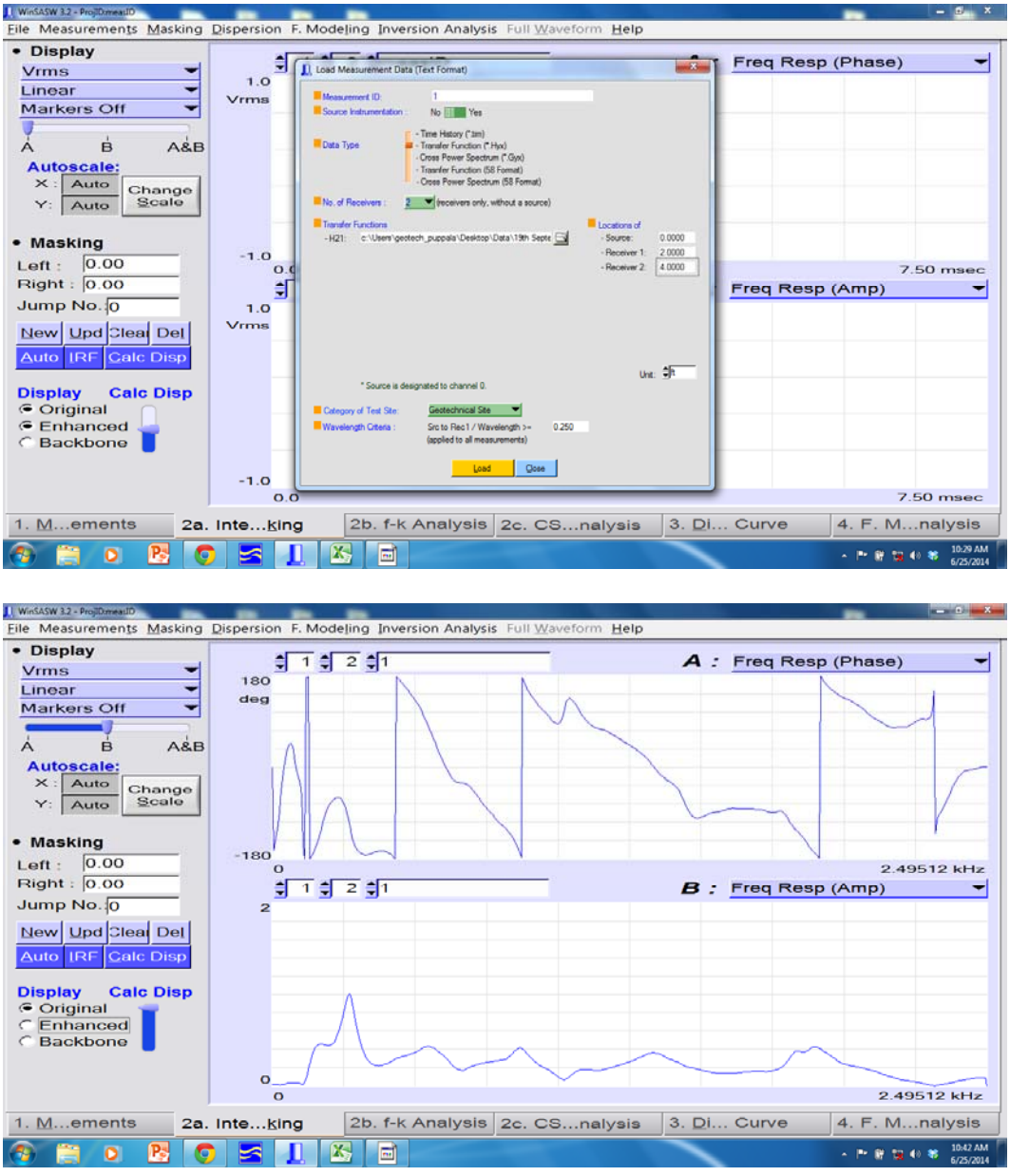

Figure 5- 7 Importing SASW data

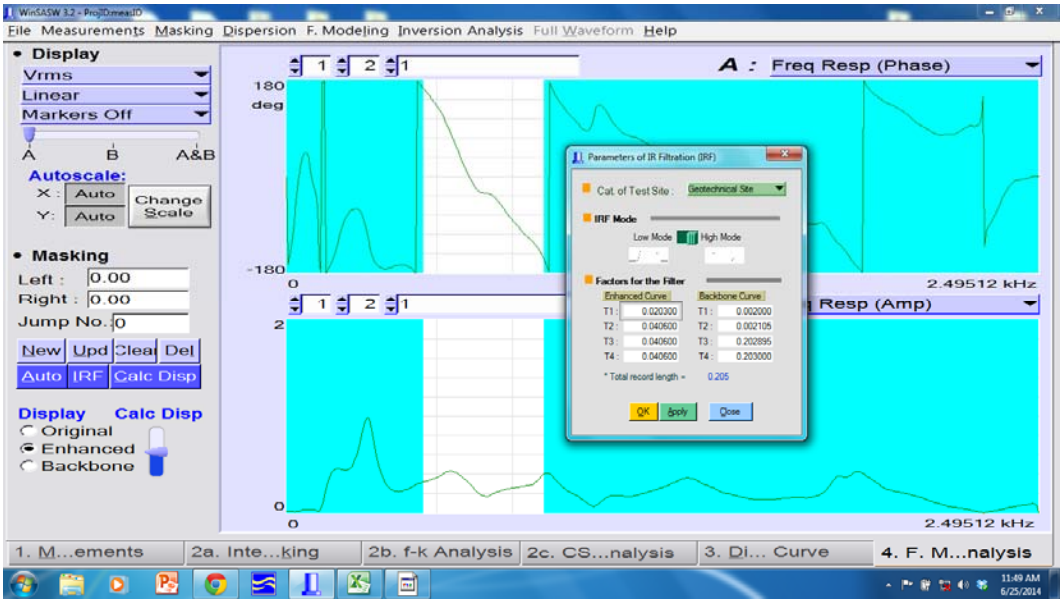

Figure 5- 8 Masking the data

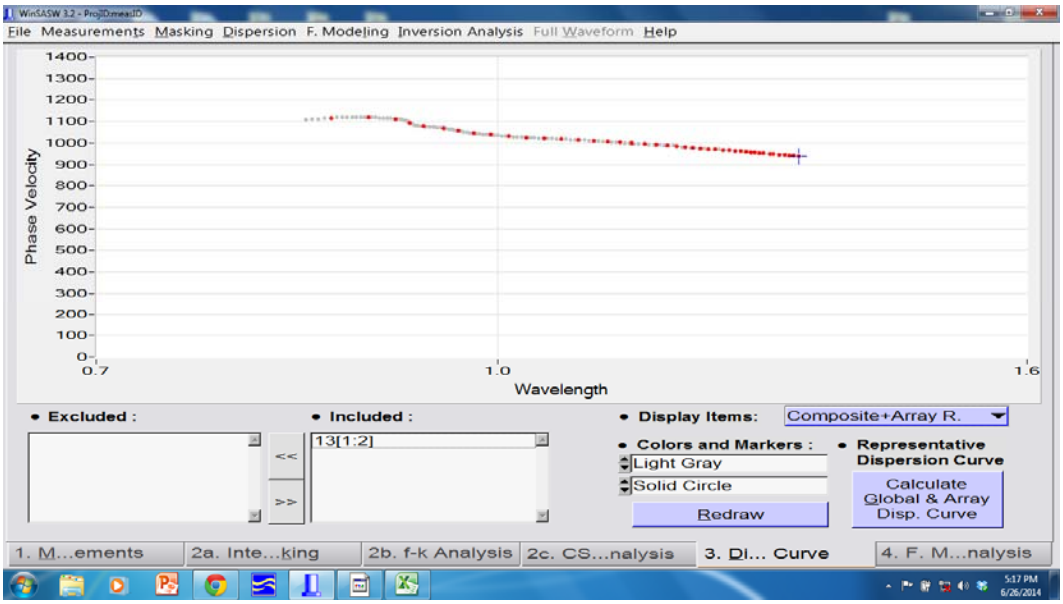

Figure 5- 9 Experimental Dispersion Curve

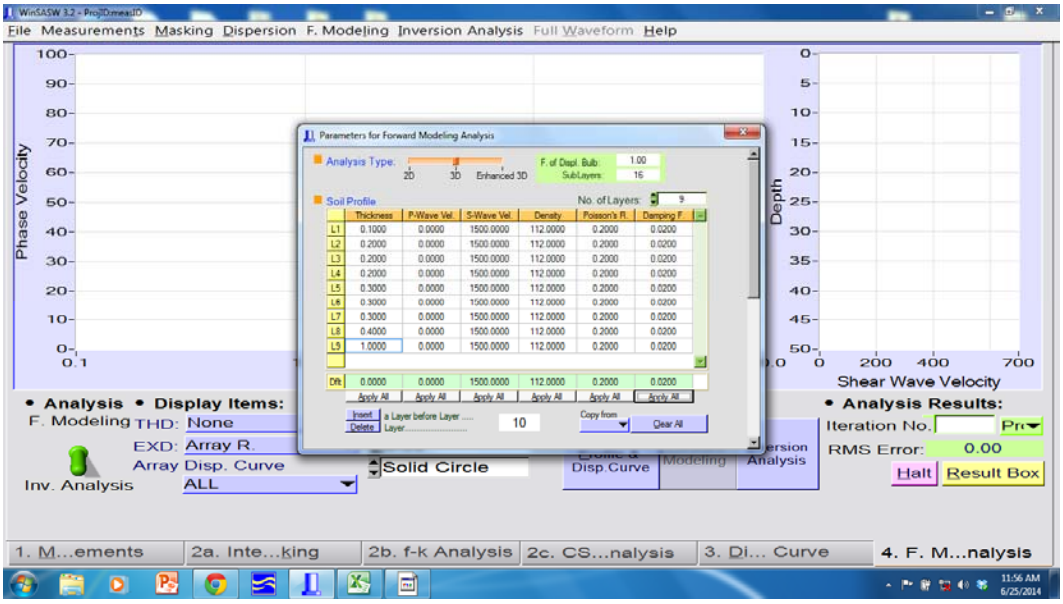

Figure 5- 10 Parameters for Theoretical Dispersion Curve

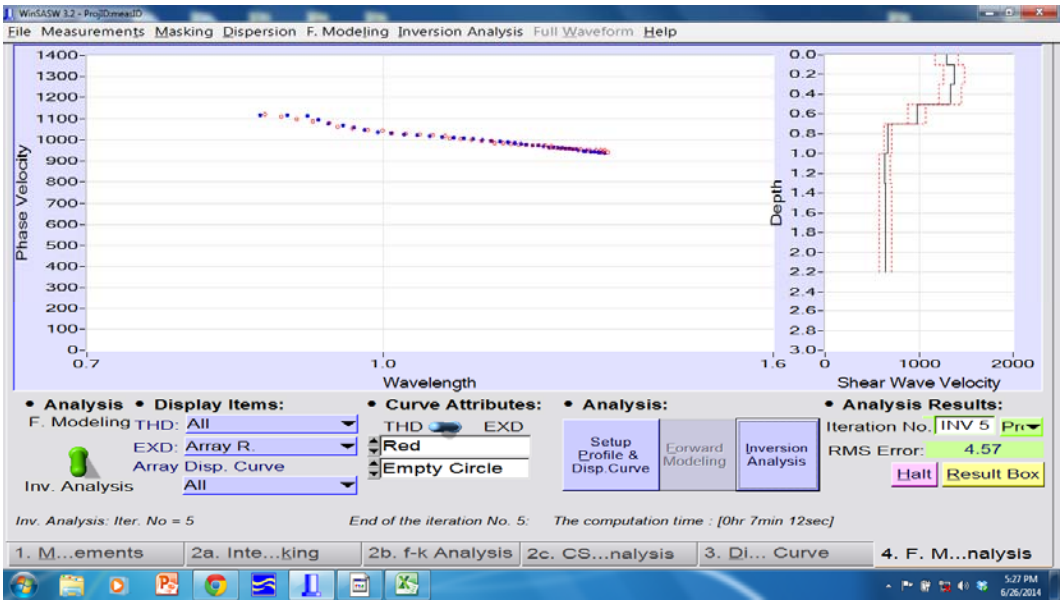

Figure 5- 11 Depth Profiling

Figure 5-12 indicates a decrease in shear wave velocity value with depth. This is interpreted to a change in the soil layer, i.e., a transition from CLSM to native soil. The value of shear wave velocity in CLSM is observed to be higher than that in the native soil because of its greater density. The decrease in shear wave velocity with depth indicates the transition between the CLSM and the native soil layer. Calculation of CLSM stiffness from the observed shear wave velocity values was accomplished by using the following formula:

$$G = \rho . V_S{}^2 \qquad (5.1)$$

where, 'ρ' is the mass density i.e. total unit weight divided by gravitational acceleration. The value for total unit weight was determined to be 18 kN/m^3 , and the value of 9.81 m/s^2 was considered as the gravitational acceleration.

5.3 SASW Test Results

The Spectral Analysis of Surface Wave test results are summarized in Tables 5-1, 5-2 and 5-3. They are followed by plots, representing the variation of shear modulus (strength) of CLSM with time. The illustrations aid in assessing the quality of CLSM over time.

Table 5- 1 Variation of CLSM Stiffness with Time for Sections 1 to 6

Section	Location	Stiffness after Day 1 (ksi)	Stiffness after Day 3 (ksi)	Stiffness after Day 7 (ksi)	Stiffness after Day 14 (ksi)	Stiffness after Day 28 (ksi)	Stiffness after Day 90 (ksi)
1 (1066-25)	South 2	-	40.1	47.4	57.8	62.7	62.9
	South 1	36.9	39.9	46.5	56.3	67.6	68.1
	Center	34.5	39.6	47.0	57.8	66.5	66.5
	North 1	36.4	41.9	47.8	56.1	64.9	65.2
	North 2	-	39.4	46.4	56.7	62.7	63.2
2 (1067-10)	South 2	-	39.4	46.7	53.7	60.6	60.8
	South 1	38.4	44.0	52.2	57.8	67.2	67.4
	Center	36.8	38.7	46.2	54.2	60.1	60.3
	North 1	34.9	37.9	40.8	57.7	66.7	67.0
	North 2	-	37.2	44.2	49.5	59.3	59.5
3 (1067-40)	South 2	-	41.4	48.8	57.3	68.7	68.9
	South 1	35.6	39.8	46.3	59.2	66.1	66.4
	Center	40.3	44.8	47.8	53.8	63.4	63.6
	North 1	39.3	50.2	56.1	59.5	65.4	65.7
	North 2	-	39.8	46.8	56.4	68.2	68.4
4 (1068-25)	South 2	-	36.4	43.7	54.0	66.1	66.2
	South 1	36.4	37.4	43.9	53.2	59.1	59.4
	Center	36.7	40.9	48.4	55.5	63.4	63.6
	North 1	37.0	39.8	42.8	50.4	59.5	59.8
	North 2	-	36.6	43.6	56.6	64.7	64.9
5 (1069-10)	South 2	-	38.0	45.3	56.2	64.1	64.3
	South 1	36.4	36.8	43.4	56.5	61.1	61.3
	Center	37.6	47.9	55.4	60.7	63.9	64.0
	North 1	38.5	43.1	50.2	57.1	60.6	60.8
	North 2	-	33.8	40.7	61.4	63.8	64.0
6 (1069-40)	South 2	-	44.6	52.0	57.6	60.9	61.1
	South 1	36.7	42.3	48.8	60.3	66.1	66.4
	Center	37.3	42.6	50.0	58.1	64.3	64.6
	North 1	35.5	37.7	43.6	56.4	65.9	66.2
	North 2	-	39.6	46.6	57.0	62.0	62.2

Table 5- 2 Table Variation of CLSM Stiffness with Time for Sections 7 to 12

Section	Location	Stiffness after Day 1 (ksi)	Stiffness after Day 3 (ksi)	Stiffness after Day 7 (ksi)	Stiffness after Day 14 (ksi)	Stiffness after Day 28 (ksi)	Stiffness after Day 90 (ksi)
7 (1070-10)	South 2	-	42.6	49.9	56.6	63.1	63.2
	South 1	37.2	37.9	43.7	57.1	64.5	64.8
	Center	37.6	37.9	45.4	57.9	65.6	65.8
	North 1	40.1	42.7	46.0	57.6	63.7	64.0
	North 2	-	40.1	47.0	59.1	63.0	63.2
8 (1070-25)	South 2	-	40.0	47.4	52.5	64.8	64.9
	South 1	36.6	39.0	45.5	51.6	68.4	68.6
	Center	36.4	40.0	47.4	59.1	65.7	66.0
	North 1	37.0	39.9	48.7	55.2	66.7	67.0
	North 2	-	38.4	45.3	56.0	64.1	64.3
9 (1070-50)	South 2	-	31.3	38.6	53.0	58.6	58.7
	South 1	-	31.7	41.2	57.0	58.7	59.0
	Center	-	32.8	41.7	54.6	58.8	59.0
	North 1	-	31.2	42.9	55.0	58.1	58.4
	North 2	-	32.8	44.1	56.0	58.5	58.7
10 (1071-10)	South 2	-	35.4	42.7	52.1	61.6	61.8
	South 1	38.5	39.6	46.2	53.2	60.1	60.3
	Center	36.0	37.1	44.6	58.0	65.7	66.3
	North 1	39.6	44.2	50.1	57.6	63.9	64.2
	North 2	-	37.2	44.1	62.1	61.0	61.2
11 (1071-40)	South 2	-	35.4	42.7	52.1	61.6	61.8
	South 1	38.5	39.6	46.2	53.2	60.1	60.3
	Center	36.0	37.1	44.6	55.1	59.9	60.5
	North 1	39.6	44.2	50.1	53.2	63.9	64.2
	North 2	-	37.2	44.1	54.8	61.0	61.2
12 (1071-50)	South 2	-	41.1	48.4	55.1	57.1	57.3
	South 1	-	35.8	42.3	50.7	53.5	53.9
	Center	-	38.7	46.2	53.2	55.5	55.7
	North 1	-	38.7	44.6	51.2	54.2	54.5
	North 2	-	40.1	47.0	56.2	57.5	57.7

Table 5- 3 Variation of CLSM Stiffness with Time for Sections 13 to 17

Section	Location	Stiffness after Day 1 (ksi)	Stiffness after Day 3 (ksi)	Stiffness after Day 7 (ksi)	Stiffness after Day 14 (ksi)	Stiffness after Day 28 (ksi)	Stiffness after Day 90 (ksi)
13 (1072-25)	South 2	-	40.0	47.3	54.8	67.0	67.2
	South 1	31.6	37.7	44.3	57.3	66.4	66.6
	Center	36.1	42.6	48.6	55.9	60.9	60.9
	North 1	39.7	40.1	46.0	55.1	62.8	63.0
	North 2	-	37.0	44.0	60.2	66.9	67.1
14 (1073-10)	South 2	-	31.5	38.8	53.4	60.8	61.0
	South 1	37.7	42.2	45.8	55.7	63.6	63.9
	Center	36.8	41.5	44.6	51.8	62.2	62.3
	North 1	35.4	39.2	42.2	57.9	62.4	62.6
	North 2	-	43.2	50.2	56.1	60.7	60.9
15 (1073-40)	South 2	-	37.5	44.8	55.7	66.2	66.4
	South 1	33.7	40.3	45.4	55.3	66.5	66.8
	Center	36.5	40.6	48.1	57.9	64.2	64.4
	North 1	42.5	43.6	49.5	55.3	68.2	68.5
	North 2	-	39.0	46.0	59.0	67.5	67.7
16 (1074-10)	South 2	-	45.1	52.4	57.5	65.2	65.4
	South 1	35.6	41.6	48.2	58.0	69.4	69.6
	Center	35.8	40.5	45.1	52.6	60.9	61.6
	North 1	37.7	39.9	45.8	52.2	67.9	68.2
	North 2	-	38.3	45.3	58.7	65.3	65.5
17 (1075-25)	South 2	-	37.5	44.8	55.7	66.2	66.4
	South 1	35.1	40.3	45.4	53.9	66.5	66.8
	Center	36.5	40.6	48.1	53.6	64.2	64.3
	North 1	42.5	43.6	49.5	58.2	68.2	68.5
	North 2	-	39.0	46.0	60.4	67.5	67.7

The results indicated an increasing trend from left to right in the tables above. This implies a strength increase of CLSM with time. The results of Section 9 and Section 12, in Table 5-1(b), represent joints in the pipeline. They have been distinguished in order to check if they (joints) induce low shear wave velocity values. It was observed that the

results in Sections 9 and 12 were slightly on the lower side at the end of 3 months (90 days), but the difference in shear wave velocity values was not significant. For better understanding, a few sections have been graphically illustrated in Figures 5-13 to 5-17.

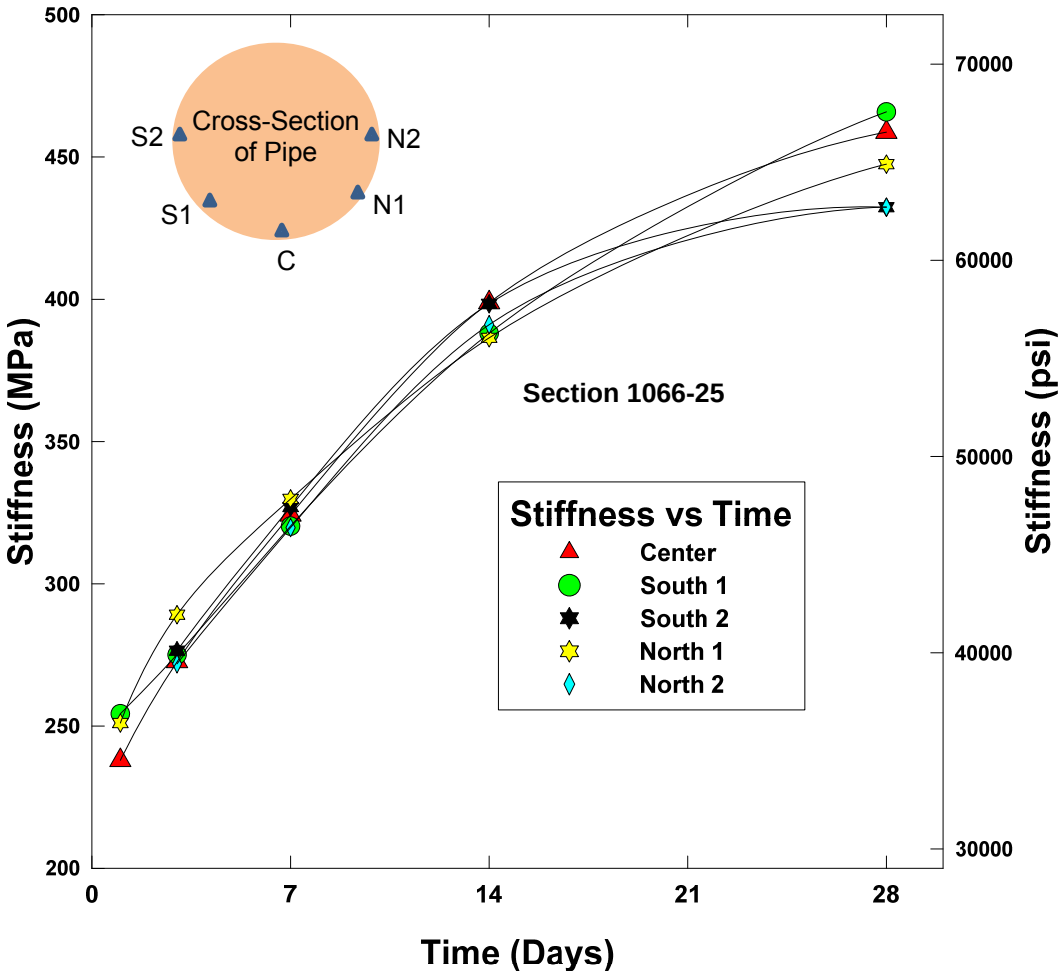

Figure 5- 12 CLSM strength for 28 days at Section 1066-25

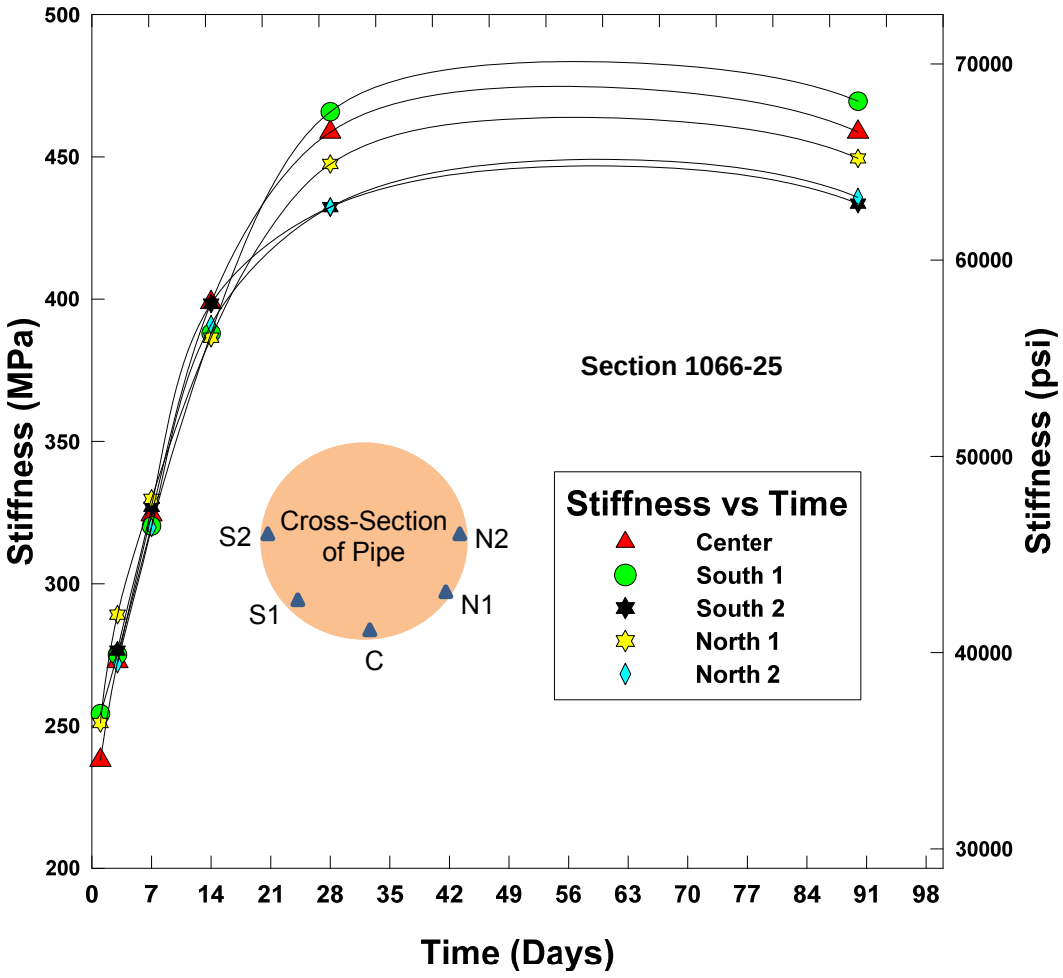

Figure 5- 13 Variation of CLSM strength for 90 days at Section 1066-25

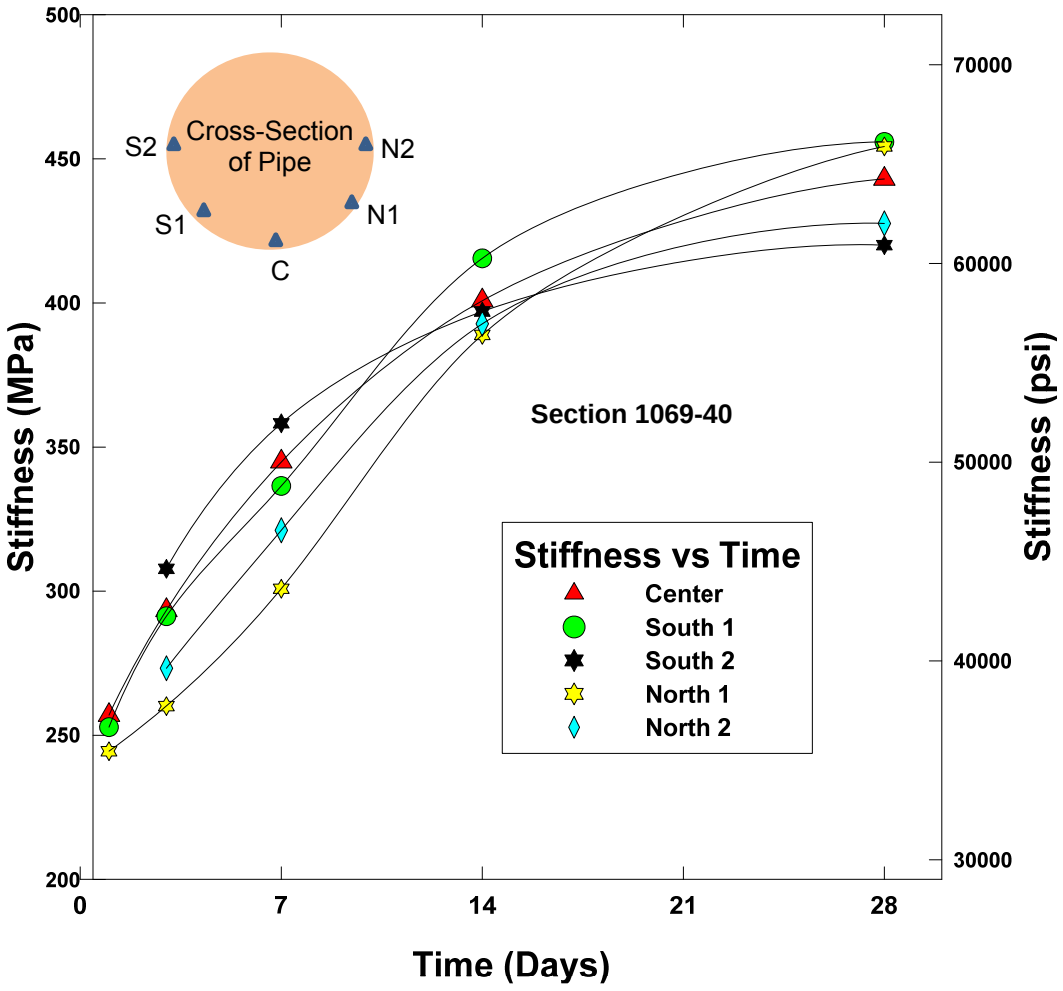

Figure 5- 14 CLSM strength for 28 days at Section 1069-40

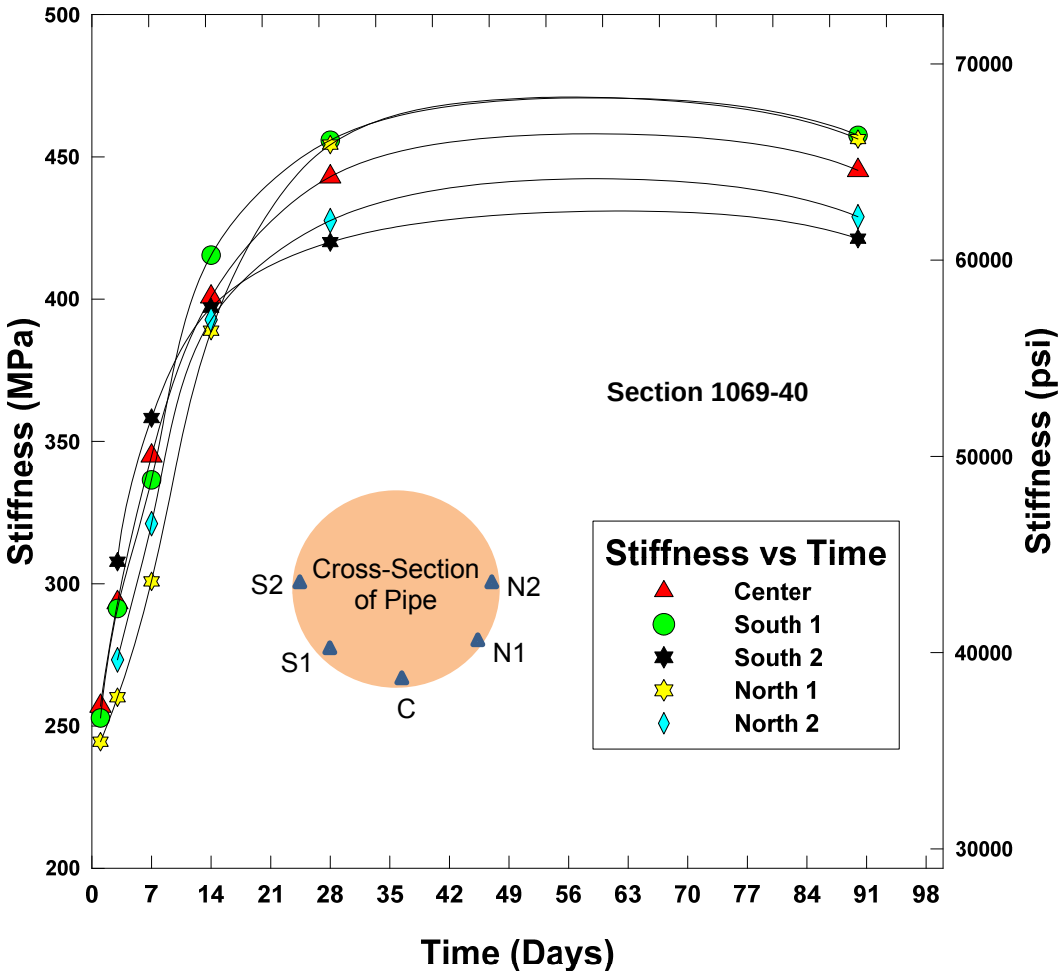

Figure 5- 15 Variation of CLSM strength for 90 days at Section 1069-40

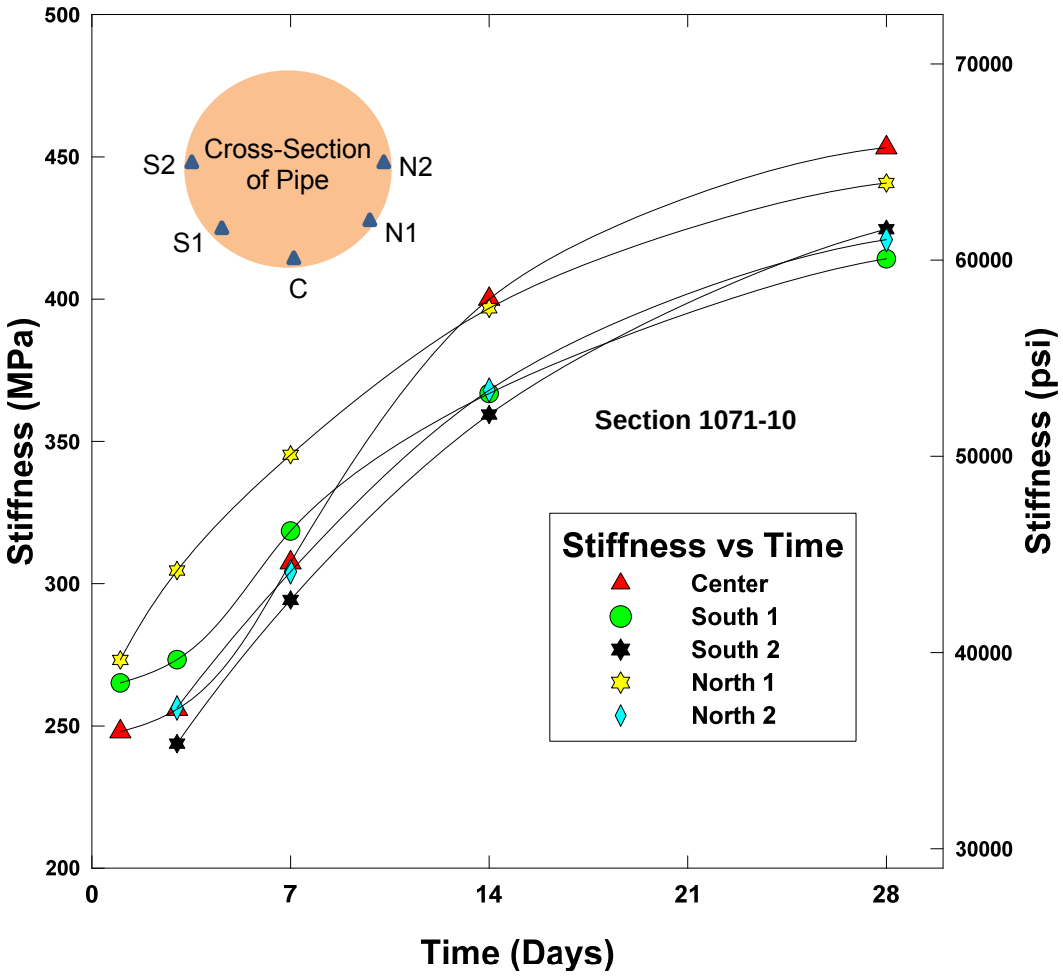

Figure 5- 16 CLSM strength for 28 days at Section 1071-10

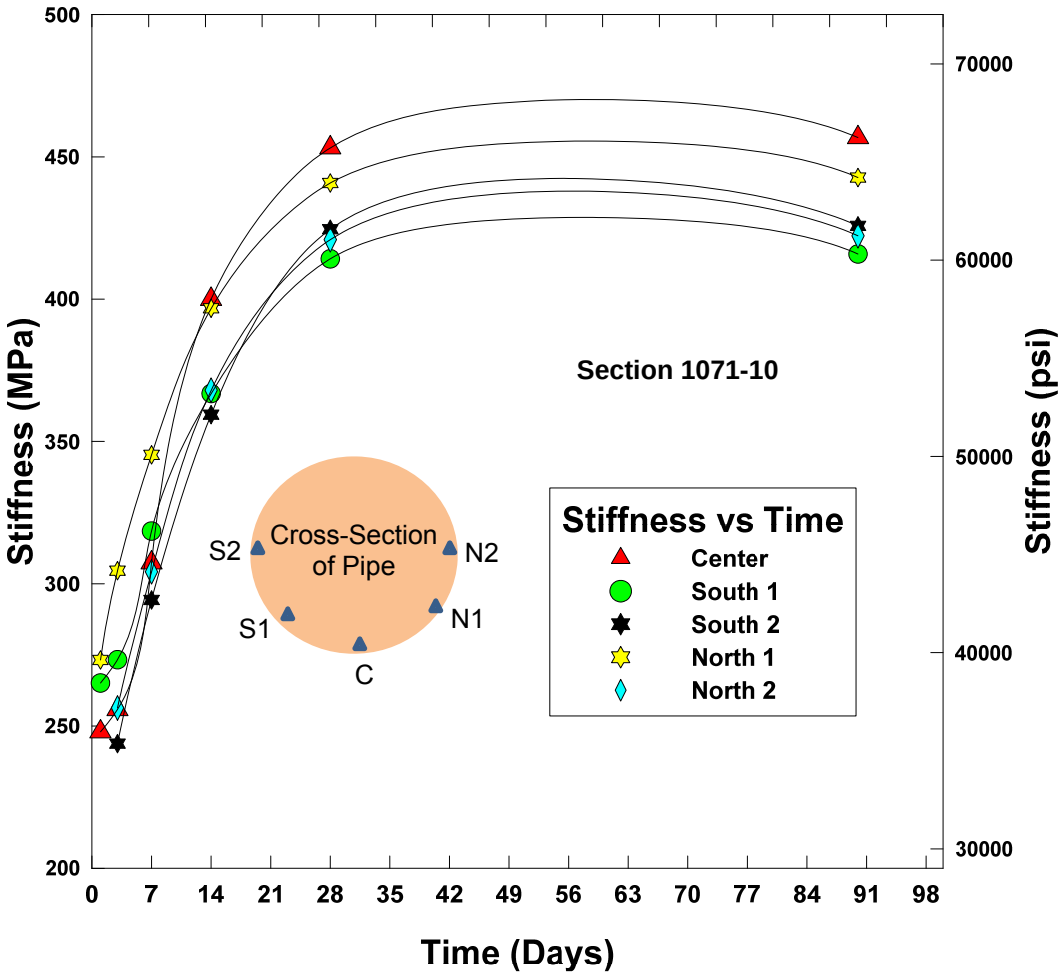

Figure 5- 17 Variation of CLSM strength for 90 days at Section 1071-10

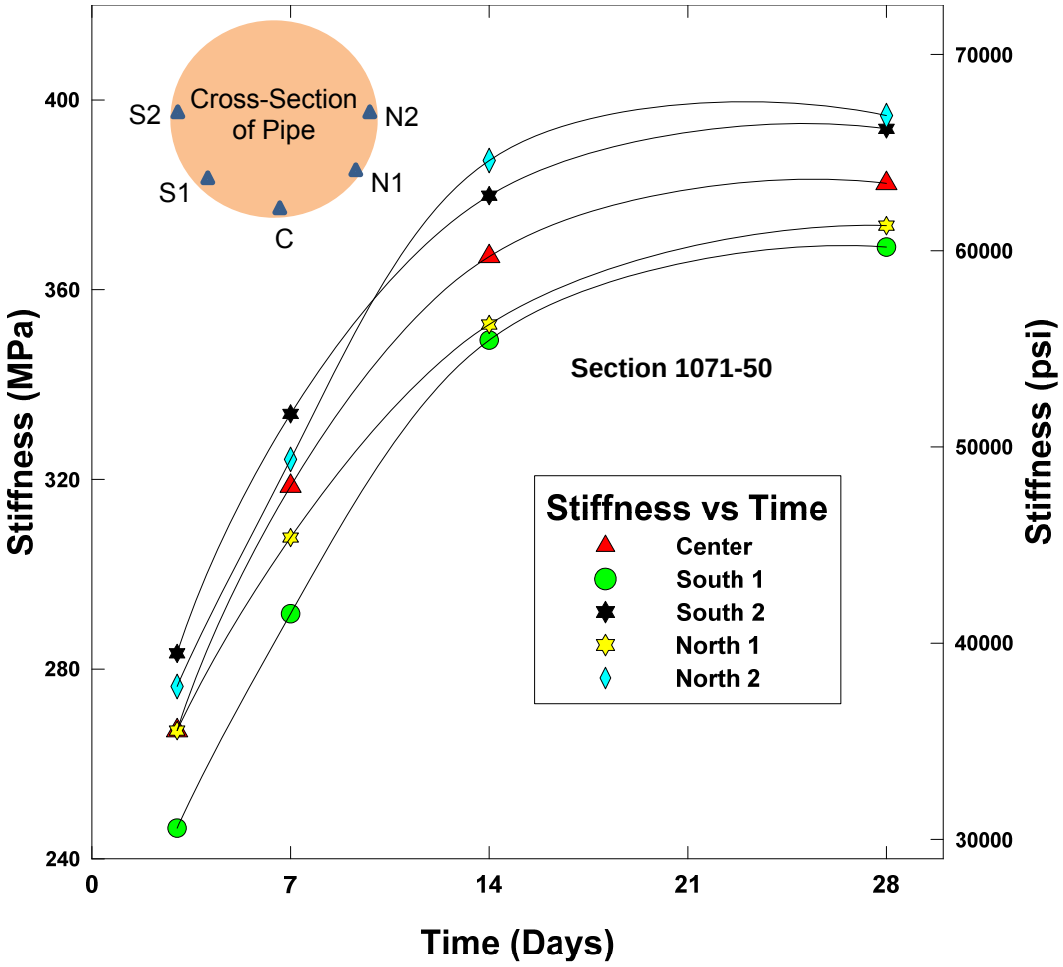

Figure 5- 18 CLSM strength for 28 days at Section 1071-50

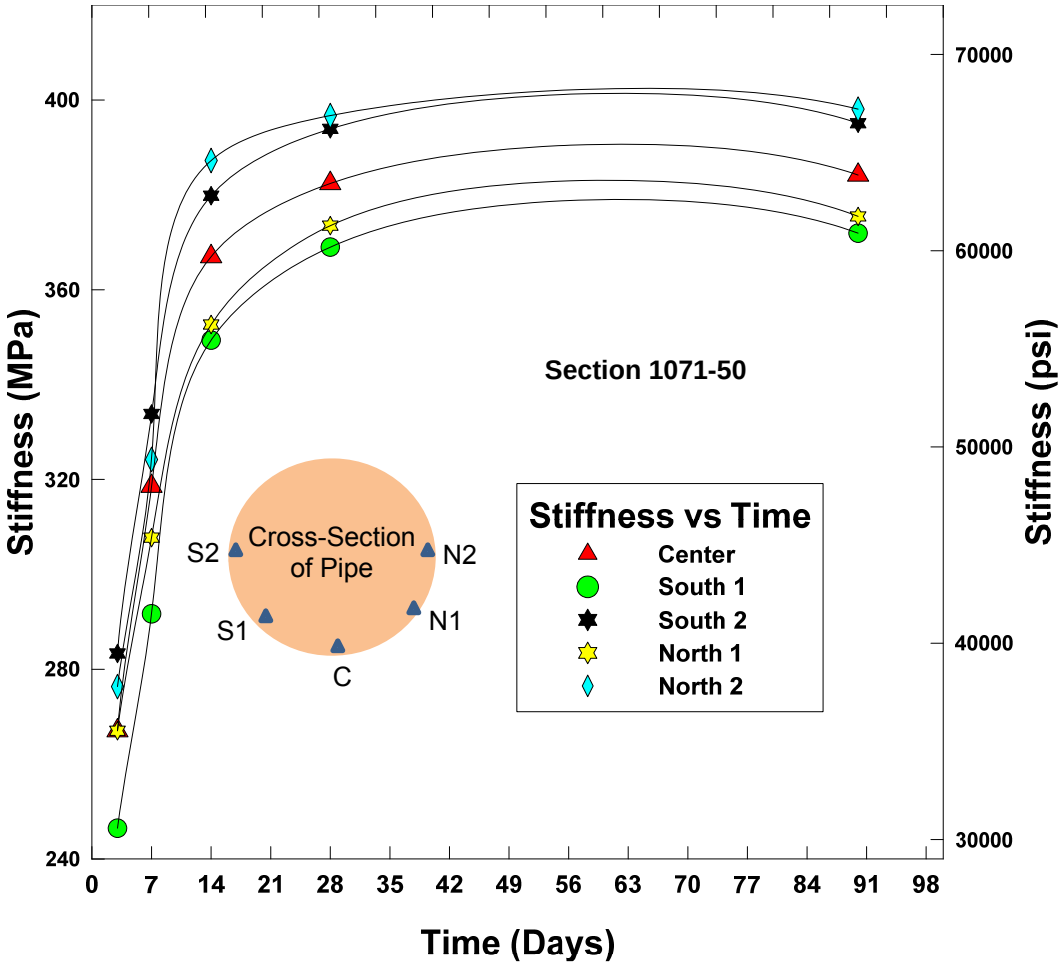

Figure 5- 19 Variation of CLSM strength for 90 days at Section 1071-50

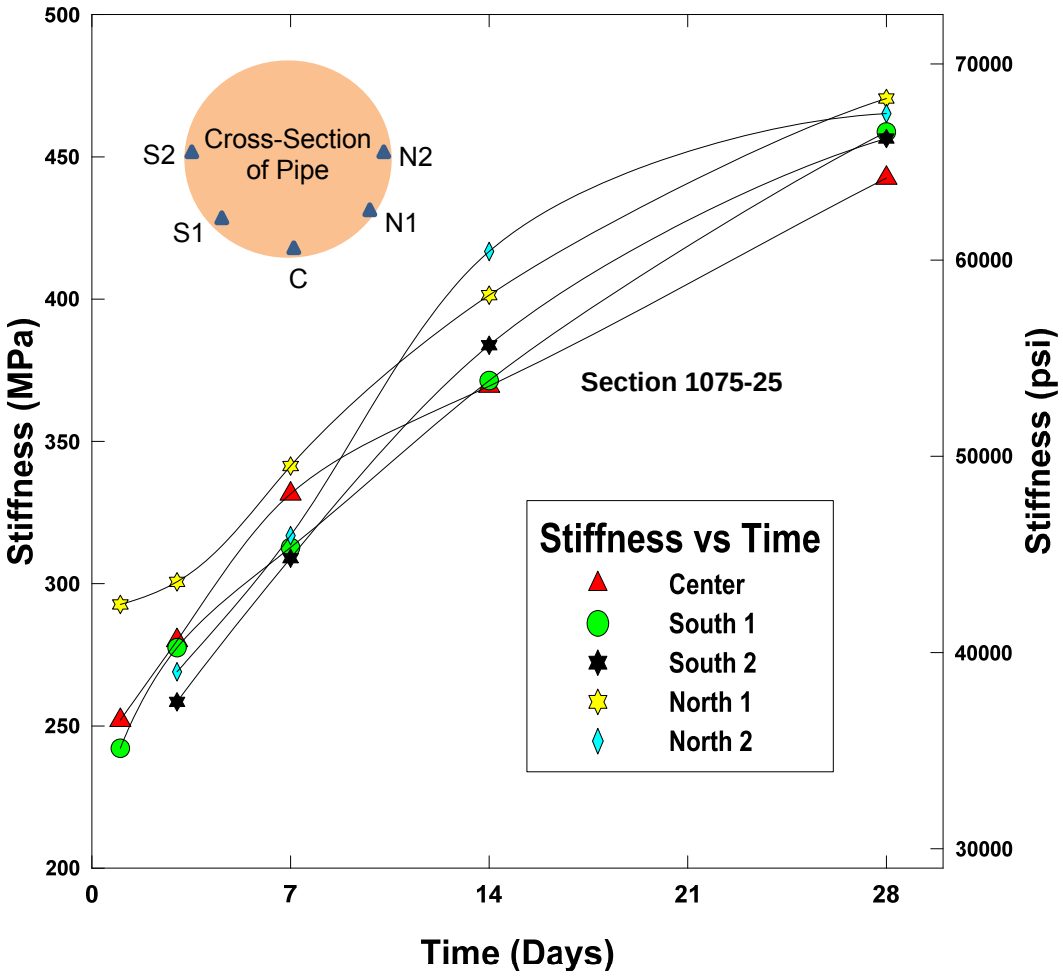

Figure 5- 20 CLSM strength for 28 days at Section 1075-25

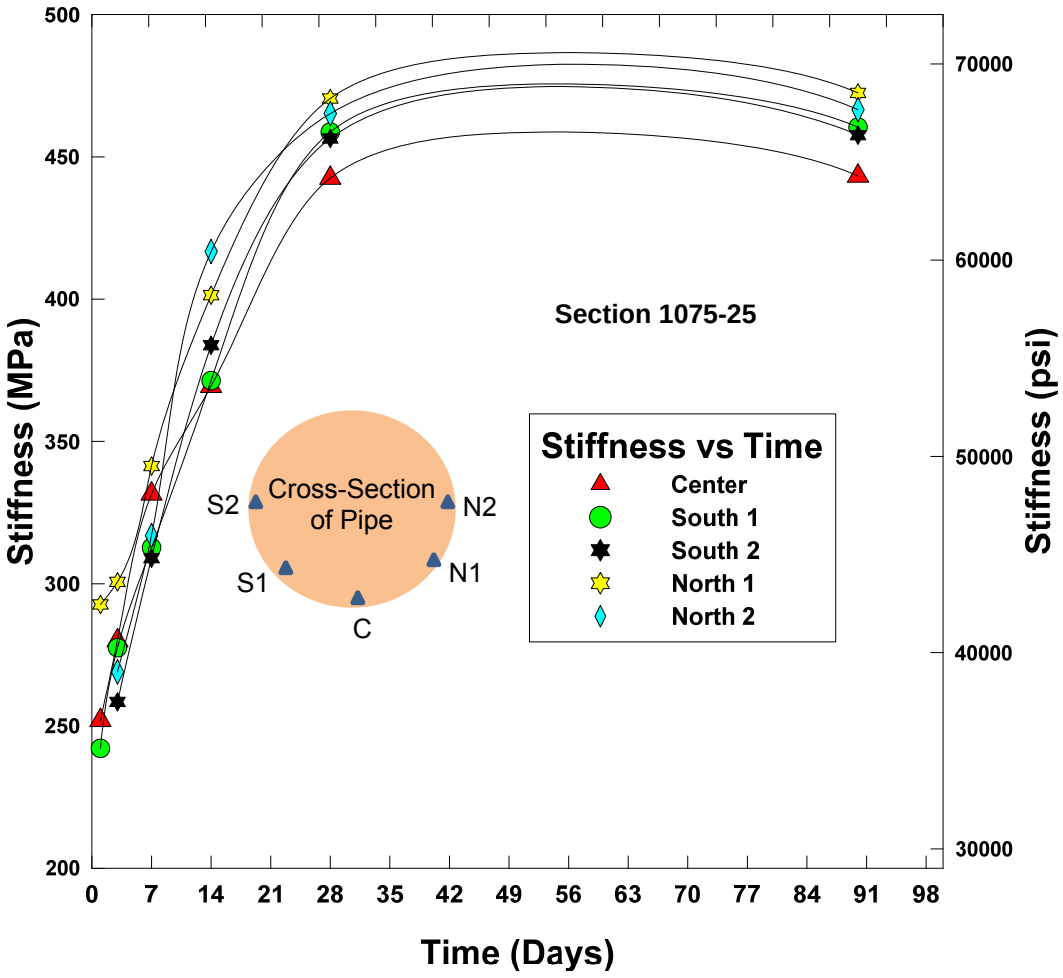

Figure 5- 21 Variation of CLSM strength for 90 days at Section 1075-25

A close observation of the results indicates that, there has been a consistent increase in strength from Day 1 to Day 28, but the rate of increase in strength of CLSM from Day 29 to Day 90 was not significant. This suggests that CLSM had attained most of its strength (approximately 90%) by the end of 28 days. Plots for the remaining sections are presented in the appendix.

5.4 Comparison Study of Field and Laboratory Test Results

A comparison study was conducted for the results of the field to that of the Resonant Column test in the laboratory. The results are summarized in Table 5-4. A graphical illustration of the comparison study is presented in Figure 5-23.

Table 5- 4 Comparison between Resonant Column and SASW Test Results

Time (days)	Resonant Column Test		SASW Test	
	V_s (m/s)	G (MPa)	V_s (m/s)	G (MPa)
1	333.7	200.5	376.8	255.8
3	357.9	230.7	392.0	276.8
7	380.1	260.3	426.9	328.3
14	408.3	300.3	452.0	368

Test results show that both the test results indicated an increase in shear modulus with time. The results obtained from the Resonant Column test in the laboratory were lower than those obtained from the SASW test in the field, for the respective days. This could be due to the difference in the environmental and physical conditions in the laboratory and the field. The CLSM in the field is under a state of greater compaction

when compared to the specimen in the laboratory. Also, the change in environmental factors like rain, temperature and moisture content contribute vitally to the variations of stiffness of CLSM. Considering the variations in these parameters for both the tests, it is acceptable to have a difference in the measured value.

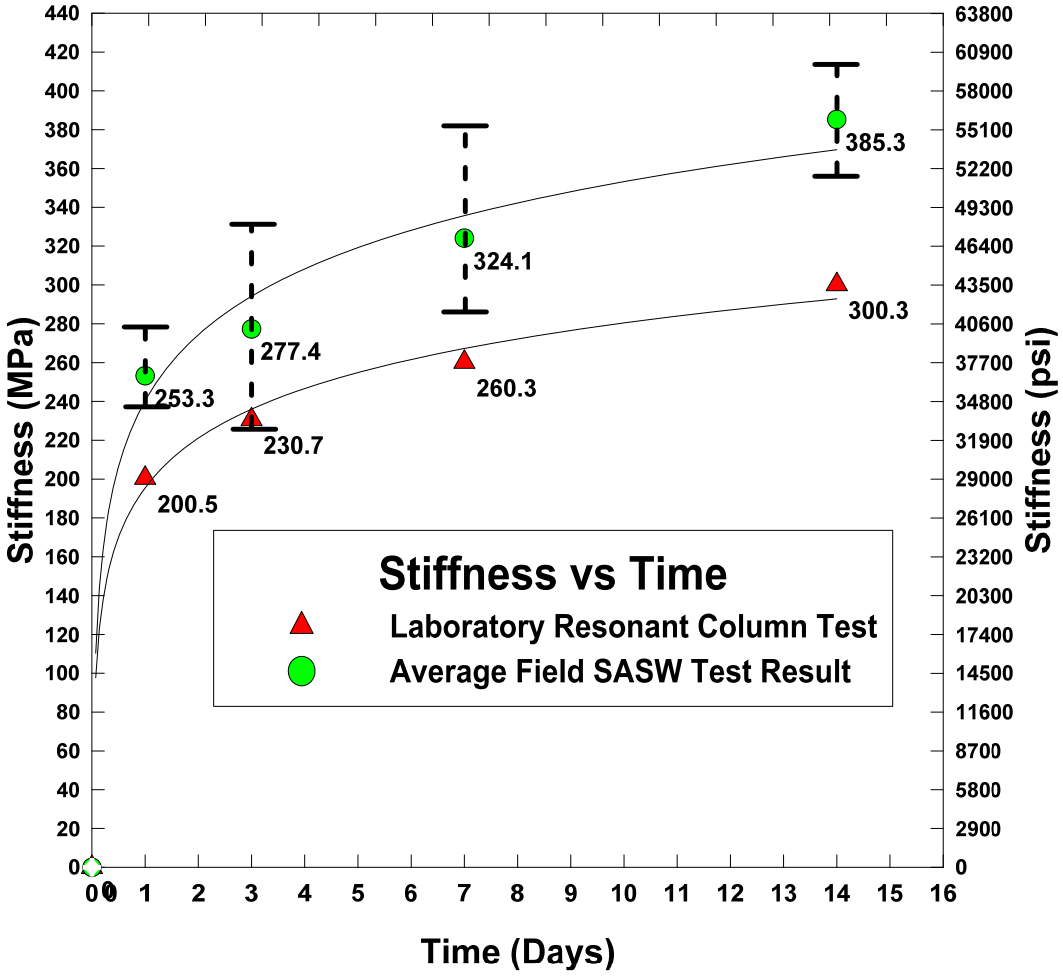

Figure 5- 22 Comparison of the variation of stiffness with time for RC and SASW Tests

E_{Secant} was determined from the UCS test in the laboratory for 50% of peak strength. E_{SASW} was calculated from the shear modulus values obtained from the SASW test results. A ratio between E_{Secant} and E_{SASW} was considered for the available time periods (days 1 to 28). A probabilistic ratio was determined and used to back calculate the UCS results. Table 5-5 illustrates an increasing trend in the predicted UCS results. The TRWD recommended strength ranged between 70 psi and 150 psi. From the predicted UCS results, CLSM has attained the recommended strength by the end of 7 days of curing. This is in close proximity of the laboratory UCS results.

Table 5- 5 Prediction of UCS from SASW Results

Time (days)	UCS Results (psi)	E_{Secant} (psi)	E_{SASW} (psi)	E_{Secant}/E_{SASW}	ProbabilisticRatio	Predicted UCS (psi)
1	5.8	517.7	88156.2	0.0059	0.085	57.7
3	14.1	1466.0	96550.7	0.0152	0.085	63.2
7	**65.3**	**8484.9**	**112826.2**	**0.0752**	**0.085**	**73.8**
14	134.8	13349.2	134110.9	0.0995	0.085	87.7
28	150.5	62587.0	150381.1	0.4162	0.085	98.4

5.5 Summary

This chapter presents the analysis of test results obtained from field investigation studies. CLSM strength improvement over time by using the shear wave velocity (V_s) and shear modulus (G) has been validated successfully. The Resonant Column test aids in providing a basis for comparing the field SASW test results.

The analyses of the SASW test, by both WinTFS and WinSASW, have been elucidated with examples and illustrations of the step-by-step procedures. Subsequently, the results of the SASW test have been tabulated, and plots of a select few sections have

been presented. A comparison study between the field SASW test results and the Resonant Column test results in the laboratory were presented in a tabulated and graphical manner. From the analysis of results, the strength of CLSM was found to increase until 28 days after setting, This inculcates the high quality of CLSM with respect to its strength.

Chapter 6

Conclusions and Recommendations

6.1 Introduction

In the current study, seismic non-destructive studies, using the Spectral Analysis of Surface Wave (SASW) method, was utilized to assess the quality of Controlled Low Strength Material (CLSM) as a potential pipeline embedment material. The quality of CLSM was assessed by monitoring the strength improvement of CLSM with time, with the help of the SASW method. The SASW results were validated by the Resonant Column test, with shear modulus as the evaluation parameter. The SASW method was performed in the field, while the UCS and Resonant Column tests were performed in the laboratory.

Samples collected from the field were studied for the UCS test. Inorder to check the consistency of the results obtained from the SASW tests in the field, replicate samples were cast in the laboratory and studied for Resonant Column test. The casting of the mix design in the laboratory was in accordance with studies conducted by Raavi (2012).

The analysis of the SASW data was performed using WinTFS and WinSASW software. WinTFS version 2.6, by Olson Instruments, Inc., and WinSASW version 3.2.12 were employed in this research. WinTFS software provided an average shear wave velocity value throughout the thickness of the subsurface layer. WinSASW provided a clear variation of shear wave velocity value, with depth.

The individual test results were summarized in tabular form. Results for the comparative study between field and laboratory tests were illustrated graphically.

6.2 Conclusions

Based on the experimental results and analyses provided in this research, the following conclusions are set forth:

1. In the current study, native low plasticity clay which is non-workable as a fill material was modified, using cement admixture, and utilized as a bedding material for a pipeline.
2. Along the pipeline, 17 test sections were selected and the SASW test was conducted at 5 points along each section.
3. The Unconfined Compressive Strength tests conducted on CLSM mixes indicated an increase in shear strength, with the increase in time. These tests also yielded the target strength after 7 days of cast of CLSM, as recommended by TRWD for this project which is 70 to 150 psi after 28 days.
4. Seismic studies in the field, using the SASW method, indicated an increase in shear modulus of CLSM with time. The shear modulus was observed to increase until day 28 and no significant variation is observed thereafter. This implies that the CLSM had gained most of its strength in 28 days after cast.
5. In order to validate the field test studies, Resonant Column test was employed to study lab cast CLSM samples. Test results indicated an increase in shear modulus with time. These results are in good agreement with the SASW test results.
6. Comparison studies conducted to determine UCS results from the SASW test results illustrated that CLSM gained the required strength by the end of 7 days of cast.

6.3 Recommendations

Based on the experiments and analyses conducted in this research, the following recommendations were suggested for future research activities:

1. Correlations demonstrating the relationship between strength of CLSM from UCS tests and stiffness of CLSM from SASW tests should be developed. This will guide contractor in estimating the strength of CLSM from its stiffness measurements in the field.
2. Laboratory techniques like Bender Element tests can be performed to validate and substantiate the field SASW results.
3. The SASW tests were performed on low plasticity clays in the current research. Tests must be performed on diverse soils to validate the consistency of CLSM as a pipeline embedment material.

References

Aouad, M.F., 1993. “Evaluation of flexible pavements and subgrades using the spectral analysis of surface waves (SASW) method”. Ph.D. Thesis, The University of Texas at Austin. p. 15.

Arshad, A. S., 005, “*Classification and Characterization of Rock Engineering Geology at JKR Quarry, Bukit Penggorak Kuantan, Pahang Darul Makmur*”: Unpublished B.S. Thesis, Geology Program, National University of Malaysia, Bangi, 94 p.

Ballard, R.F., Jr, 1964. “Determination of Soil Shear Moduli at Depth by In Situ Vibratory Techniques”. Miscellaneous Paper No. 4-691, U. S. Army Engineer Waterways Experiment Station, Vicksburg, Mississippi.

Bay, J.A., Stokoe II K.H., 1990. “Field determination of stiffness and integrity of PCC members using the SASW method”. *In: Proceedings of nondestructive evaluation of civil structures and materials conference*, University of Colorado, Boulder. p. 71-86.

Bowen, B.R., Stokoe II K.H., 1992. “Evaluation of cracked and repaired beams and columns using surface stress waves”. *In: Proceedings of the 10th World Conference on Earthquake Engineering*, Madrid, Spain.

Braile, L.W., 2010. “Seismic Waves and Slinky: A Guide for Teachers.” Department of Earth and Atmospheric Sciences, Purdue University.

Chittoori, Bhaskar; Puppala, Anand: Pedarla, Aravind, 2014. “Durability Studies on Native Soil Based Controlled Low Strength Material.” ASCE, Ground Improvement and Geosynthetics GSP 238.

Cho, Y. S. and Lin, F. B., 2001, “Spectral analysis of surface wave response of multi-layer thin cement mortar slab structures with finite thickness”: *NDT&E (Nondestructive Testing and Evaluation) International*, Vol. 34, pp. 115-122.

Chun-Hung Lin and Chih-Ping Line, 2012. “Metamorphosing the SASW Method by 2D Wavefield Transformation.” J. Geotech. Geoenviron. Eng., 138(8), 1027-1032.

Deere, D. U., 1964, “Technical description of cores for engineering purpose”: *Rock Mechanics Engineering Geology*, Vol. 1, pp. 16-22.

Deere, D. U., 1968, Geological considerations. In Stagg, R. G. and Zienkiewicz, D. C. (Editors), *Rock Mechanics in Engineering Practice*: Toby Wiley and Sons, New York, pp 1-20.

Goh, T. L., Abdul Rahim Samsudin, Abdul Ghani Rafek, 2011, “Application of Spectral Analysis of Surface Wave Method for Rock Mass Characterization”: *Environmental & Engineering Geoscience, Vol. XVII*, No. 1, pp. 77-84.

Groves, Paul, 2010. “Applications of Nondestructive testing in Civil Engineering.” M.S. Thesis, University of Waterloo, Canada.

Gucunski, M., 1991. “Generation of low frequency Rayleigh waves for the spectral analysis of surface waves method”. Ph.D. Thesis, Ann Arbor: Department of Civil and Environmental Engineering, University of Michigan.

Gucunski, N., Woods, R.D., 1992. “Numerical simulation of the SASW test”. Soil Dynamics and Earthquake Engineering 11 (4), 213-227.

Haskell, N.A., “The Dispersion of Surface Waves in Multilayered Media”. *Bulletin of the Seismological Society of America*, Vol. 43, 17-34.

Heisey, J.S., Stokoe II K.H., Meyer A.H., 1982. “Moduli of pavement systems from spectral analysis of surface waves”. *Transportation research record*, No. 852, Washington, DC. p. 22-31.

Hitunen, D.R., 1988. “Experimental evaluation of variables affecting the testing of pavements by the spectral analysis of surface waves method”. Ph.D. Thesis, Ann Arbor: Department of Civil Engineering, University of Michigan.

Houlsby, G.T., 1981. “A Study of Plasticity Theories and their applicability to Soils.” Ph.D. Thesis, University of Cambridge.

Jones, R., 1962. “Surface Wave Technique for Measuring the Elastic Properties and Thickness of Roads: Theoretical Development,” British Journal of Applied Physics, Vol. 13, 21-29.

Jones, R.B., 1958. “In situ measurements of the dynamic properties of soil by vibration methods”. Geotechnique 46 (2), 357-362.

Jongwan Eun and Junhwan Lee, 2012. “Effect of Soil Parameters on Elastic Characteristics of Subgrade Materials.” J. Mater. Civ. Eng., 24 (4), 409-417.

Jyant Kumar ad Sutapa Hazra, 2014. “Effect of Input Source Energy on SASW Evaluation of Cement Concrete Pavement.” J. Mater. Civ. Eng., 26(6), 04014013.

Leo J. Peters, 1949. “The direct approach Magnetic Interpretation and its practical application,” 14(3), 290-320.

Malhatra, V.M., Carino J, 1991. CRC handbook on “nondestructive testing of concrete”. Boca Raton, Florida (FL): CRC Press, Inc.

Merino, G.J.J. et al., 2012. “Automatic picking in the refraction microtremor (ReMi) technique using morphology and color processing.” Soil Dynamics and Earthquake Engineering, Vol. 42, p. 95-104.

Murillo, C.A., Thorel Luc, Caicedo Bernardo, 2009. “Spectral analysis of surface wave method to assess the shear wave velocity within centrifuge models”. *Journal of Applied Geophysics 68*, 135-145.

Nazarian, S. and Stokoe, K. H., II, 1984, “In situ shear wave velocity from spectral analysis of surface waves”: *Proceedings, 8th World Conference on Earthquake Engineering*, Vol. 3, pp. 31-38.

Nazarian, S., 1984. "*In situ determination of elastic moduli of soil deposits and pavement systems by spectral analysis of surface waves method*". Ph.D. Thesis, Department of Civil Engineering, The University of Texas at Austin.

Nazarian, S., Yuan D, Baker M.R., 1995. "Rapid determination of pavement moduli with spectral analysis of surface waves method". *Transportation research Report, 1243-1*. The Center for Geotechnical and Highway Materials Research, The University of Texas at El Paso.

Olson Instruments, 2012. "Spectral Analysis of Surface Waves Test SASW-S/SASW-G NDE-360," System Reference Manual.

Pyakurel, Sandeep; Halabe, Udaya B., 2008. "GPR Scanning Methods for Enhanced Data Imaging in Wooden Logs." AIP Conference Proceedings, Vol. 975 Issue 1, p1674-1681.8p.

Richart, F.E., Hall, J.R., and Woods, R.D., 1970. "Vibrations of Soils and Foundations," Prentice-Hall Inc., New Jersey.

Rix, G.J., 1988. "Experimental study of factors affecting the spectral analysis of surface waves method". Ph.D. Thesis, Department of Civil Engineering, The University of Texas at Austin.

Rosenblad, B.L., Jianhua Li, 2009. "Comparative Study of Refraction Microtremor (ReMi) and Active Source Methods for Developing Low-Frequency Surface Wave Dispersion Curves." Journal of Environmental and Engineering Geophysics, Vol. 14, Issue 3, pp. 101-113.

Sanchez-Salinero, I., 1987. "Analytical investigation of seismic methods used for engineering applications". Ph.D. Thesis, The University of Texas at Austin.

Satoh, T. et al., 1991. "Soil Profiling by Spectral Analysis of Surface Waves". Proceedings: Second International Conference on Recent Advances in

Geotechnical Earthquake Engineering and Soil Dynamics, St. Louis, Missouri, Paper No. 10.23.

Satoh, T., 1989. "On the Controlled Source Spectral Rayleigh Wave Excitation and Measurement System," VIC, Tokyo.

Sheu, J.C., 1987. "Application and limitations of spectral analysis of surface waves method". Ph.D. Thesis, Department of Civil Engineering, The University of Texas at Austin.

Stokoe II, K.H., Nazarian, S., 1983. "Effectiveness of ground improvement from spectral analysis of surface waves". Proc. *8th European Conference on Soil Mechanics and Foundation Engineering*, Helsinki, Finland, Vol. 1, pp. 91-94.

Stokoe, H.S. et al., 1988. "In Situ Testing of Hard-to-Sample soils by Surface Wave Method". ASCE Speciality Conference on Earthquake Engineering and Soil Dynamics II – Recent Advances in Ground Motion Evaluation, Park City, Utah, 264-278.

Suharsono and Samsuddin, A. R., 2003, "*The attenuation effects of surface wave propagations on rock mass using SASW method*": Bulletin Geological Society Malaysia, Vol. 46, pp. 475-478.

Suharsono, 2006, "*Application of Spectral Analysis of Surface Wave as New Technique for Rock Mass Classification in Engineering Geology"*: Unpublished Ph.D. Thesis, Geology Programme, National University of Malaysia, Bangi, 192 p.

Tallavo, F., Cascante, G., Pandey, M., 2009. "Experimental and Numerical Analysis of MASW tests for detection of buried timber trestles." Soil Dynamics and Earthquake Engineering, Vol. 29, Issue 1, p. 91-102.

Wightman, W.E., Jalinoos, F., Sirles, P., Hanna, K., 2003. “Application of Geophysical methods to Highway related Problems.” Federal Highway Administration, Lakewood, CO. Publication No. FHWA-IF-04-021.

Biographical Information

Rathna Phanindra Mothkuri was born in Hyderabad, Andhra Pradesh, India. Hailing from an orthodox Brahmin family, Rathna was well versed in ceremonial and traditional ethics, in addition to studying, sports and extra-curricular activities. His father was a Chartered Accountant by profession and his mother was an Educationist. Rathna went to Vidyaranya High School for his primary schooling and Kendriya Vidyalaya Picket for his secondary schooling. He earned his bachelors degree at the Bhaskar Engineering College in Hyderabad. Rathna was also a National Level swimmer. He was awarded a Silver medal and a Bronze medal at the Nationals in India.

Born in 1990, Rathna spent 22 years in Hyderabad before moving to the USA in 2013 to pursue a Master's degree, with a specialization in geotechnical engineering at the University of Texas at Arlington. At UTA, he had an opportunity to be a graduate research assistant under the guidance of Dr. Anand J. Puppala and to work on various research projects, such as "Integrated Pipeline (IPL) Project" funded by the Tarrant Regional Water District (TRWD), and "Pilot Implementation using Geofoam for Repair of Bridge Approach Slabs and Adjoining Roadway" funded by the Texas Department of Transportation (TXDOT).